BDNF/TrkB mediates long-distance dendritic growth by activating CREB/PI3K-mTOR-dependent translation in neuronal cell bodies.

Moya-Alvarado, G[1] and Bronfman, F.C[1,2*].

[1]Department of Physiology, Faculty of Biological Sciences. Pontificia Universidad Catolica de Chile, Santiago, Chile

[2]Center for Aging and Regeneration (CARE), Institute of Biomedical Sciences (ICB), Faculty of Medicine, Universidad Andres Bello. Santiago, Chile

*To whom correspondence should be addressed: Francisca C. Bronfman.
Email: francisca.bronfman@unab.cl. Tel: +56 226618358

Acknowledgements: The authors want to thank Carolina Ramirez for help with the compartmentalized cultures, and Nicolas Stuardo for help with BDNF monobiotinylation protocol.

Funding: The authors gratefully acknowledge financial support from ANID (Agencia Nacional de Investigacion y Desarrollo) FONDECYT grant Nº 1171137 (FB), Basal Center of Excellence in Science and Technology CONICYT (AFB170005), Millennium Nucleus (P07/011-F), and the PhD fellowship from CONICYT (GM).

ABSTRACT

Brain-Derived Neurotrophic Factor (BDNF) is broadly expressed in many circuits of the central nervous system (CNS). It binds TrkB and p75 to trigger different signaling pathways, including ERK1/2 and PI3K-mTOR, to induce dendritic growth and synaptic plasticity. When binding to BDNF, TrkB and p75 are endocytosed to signaling endosomes to continue signaling inside the cell. Whether BDNF/TrkB-p75 signaling endosomes in axons are regulating long-distance signaling in cell bodies to modify neuronal morphology is unknown. Here, we studied the functional role of BDNF signaling endosomes in long-distance regulation of dendritic growth using compartmentalized cultures of rat and mouse cortical neurons derived from $p75^{exonIII}$ knock-out or $TrkBF^{616A}$ knock-in mice. By applying BDNF to distal axons, we showed the capacity of axonal BDNF to increase dendritic arborization in cell bodies. This process depended on TrkB activity, but not p75 expression. In axons, BDNF/TrkB co-localized with Rab5 endosomes and increased active Rab5. Also, dynein was required for BDNF long-distance signaling, consistent with sorting and transport of signaling endosomes. Using neurons derived from $TrkBF^{616A}$ knock-in mice and the 1NM-PP1 inhibitor, we were able to demonstrate that TrkB receptors activated in the axons by BDNF, were required in the neuronal cell body to increase TrkB activity and phosphorylation of CREB. Also, we were able to visualize endosomes containing activated TrkB. PI3K activity was not required in the axons for dynein dependent BDNF responses. However, dendritic arborization induced by axonal BDNF signaling required both nuclear CREB and PI3K activation in cell bodies. Consistently, axonal BDNF increased protein translation in cell bodies and CREB and PI3K and mTOR activity were required for this process. Altogether, these results show that BDNF/TrkB signaling endosomes generated in axons allows long-distance control of dendritic growth coordinating both transcription and protein translation. Our results suggest a role of BDNF-TrkB signaling endosomes wiring circuits in the CNS.

INTRODUCTION

The growth of dendritic threes during central nervous system (CNS) development is an essential process for the establishment of proper connectivity (Jan and Jan, 2010). After birth, dendrites and synapsis undergo plastic changes that are required for physiological processes such as learning and memory. The morphology of the dendritic arbor is maintained and undergoes plastic changes in a process that requires activity-dependent transcription factors (TFs), protein translation, and extracellular signaling molecules (Sutton and Schuman, 2006; Wong and Ghosh, 2002; Yap and Greenberg, 2018). Brain-derived neurotrophic factor (BDNF) is a well-known gene regulated by neuronal activity. BDNF is a member of the neurotrophin family of growth factors whose expression is required for the maintenance of dendrites of adult striatal and cortical neurons (Gorski et al, 2003; Horch et al, 1999).

Furthermore, BDNF increases the dendritic branching of cortical and hippocampal neurons in dissociated cultures and organotypic slices (Cheung et al., 2007; Horch and Katz, 2002). BDNF binds two types of receptors, the tyrosine kinase receptor B (TrkB) and the pan neurotrophin receptor p75 (Huang and Reichardt, 2003; Yan et al., 1997). However, the growth-promoting action of BDNF is associated with TrkB; consistently, a mutant mouse with inducible deletion of TrkB receptors exhibit a significant reduction of dendritic arbor and neurodegeneration in cortical neurons (Xu et al., 2000).

The neuronal growth mediated by TrkB activation in neurons is triggered by signaling pathways such as ERK1/2 and PLCγ that activate the cAMP response element CRE-binding protein (CREB) (Finkbeiner et al., 1997; Xing et al., 1998, Gonzalez et al 2019), mediating activity-dependent transcription (Flavell and Greenberg, 2008; Yap and Greenberg, 2018). Also, the activation of the class 1 phosphoinositide 3-kinase (PI3K)/Akt/ and the mammalian target of rapamycin (mTOR) (Dijkhuizen and Ghosh, 2005; Minichiello et al., 2002) contribute to this process. Several lines of evidence suggest that BDNF increases the local translation of a subset of mRNAs in dendrites in a mTor dependent manner, including proteins related to CNS plasticity (Leal et al., 2014; Ravindran et al., 2019; Schratt et al., 2004; Takei et al., 2004). Thus, mTor controls dendrite size and shape in a BDNF-dependent manner via the PI3K/Akt pathway (Kumar et al., 2005).

Ligand binding of BDNF promotes TrkB internalization of ligand-receptor in endocytic organelles. A wealth amount of evidence has shown that a complex of neurotrophins and neurotrophin receptors continue signaling inside the cell in a specialized organelle named signaling endosomes, where it encounters specific signaling adaptors (Grimes et al, 1996; Bronfman et al, 2014; Debaisieux et al, 2016). Consistently, several studies have shown that endocytosis of TrkB is required for survival, dendritic arborization, and cell migration (Zheng et al., 2008; Zhou et al., 2007), suggesting that endosomal signaling has a role in the physiological responses to TrkB. We have shown that BDNF/TrkB signaling increases the activity and mobility of the Rab5 labeling early-endosomes and Rab11 labeling recycling endosomes. Rab5 and Rab11 are key Rab GTPases that regulate endosomal trafficking. In turn, the activity of these GTPases is required for BDNF-induced dendritic branching in a CREB-dependent manner (Lazo et al 2013; Moya-Alvaro et al 2018; Gonzalez et al 2019).

Due to the polarized morphology of neurons, distal dendrites and axons must communicate to the cell body for proper neuronal homeostasis. This communication is achieved by bidirectional transport of organelles in a process that requires microtubule-associated molecular motors (Bronfman et al., 2014; Hirokawa et al, 2010; Terenzio et al, 2017). It has been shown that BDNF is retrograde transported in axons of cortical neurons (Olenick et al., 2019; Zhou et al., 2012). Furthermore, endosomes containing activated TrkB are associated with the dynein adaptor snapin and, the disruption of snapin/dynein interaction decreases dendritic arborization (Zhou et al., 2012). However, few studies have addressed the long-distance effects of BDNF in the CNS (Cohen et al., 2011; Lom et al., 2002). On the other hand, long-distance communication of neurotrophins from the target tissue to cell bodies has been described in the peripheral nervous system (Harrington and Ginty, 2013; Ye et al., 2003; Cosker and Segal, 2014; Scott-Solomon and Kuruvilla, 2018). How long-distance communication is achieved in neurons, is a matter of intense research. However, the favorite hypothesis is that signaling endosomes originating in synaptic terminals propagate distal neurotrophin signals to the nucleus for transcriptional regulation (Riccio et al, 1997; Watson et al, 1999; Haihong et al, 2003). In that context, our lab and others have described that the cAMP responds elements binding protein (CREB) is phosphorylated in the nucleus of cortical neurons when BDNF is added exclusively to the axons of compartmentalized neuronal cultures (Bronfman et al., 2014; Deinhardt et al., 2006; Zhou et al., 2012), suggesting that CREB may mediate long-distance signaling by BDNF.

Here, we used compartmentalized cultures of rat and mouse cortical neurons using microfluidic chambers to study the mechanism of long-distance BDNF signaling in CNS neurons. We show that axonal stimulation with BDNF promotes dendritic growth in neuronal cell bodies. This effect was mainly dependent on TrkB, and although p75 down-regulation affected the basal morphology of neurons, it did not affect long-distance BDNF responses. As previously reported, axonal BDNF increases the activation of CREB. Consistently, we found that CREB activity was required for long-distance BDNF dendritic growth. The dendritic growth and activation of CREB by axonal BDNF dependent on dynein mediated transport of activated TrkB, suggesting that the process requires TrkB signaling endosomes transport. Supporting these results, we showed that dynein-dependent transport of TrkB from axons was needed to increase active TrkB in cell bodies. In agreement with these results, axonal endosomes carrying active TrkB were found in cell bodies.

Interestingly, PI3K activity was only needed in the cell body compartment to promote dendritic arborization and mTOR activation induced by axonal BDNF signaling. Consistently, the increase in the activity of both CREB and mTOR induced by BDNF stimulation in axons promotes somatodendritic protein synthesis in cell bodies, demonstrating that signaling endosomes coordinate transcription and translation to increase neuronal growth. Our finding suggests that there is a functional role of BDNF/TrkB signaling endosomes in regulating long-distance dendritic growth in central neurons.

RESULTS

BDNF axonal signaling promotes dendritic branching in a TrkB-dependent manner.

Using compartmentalized cultures of cortical neurons in microfluidic chambers we evaluated whether the axonal stimulation of BDNF promotes dendritic arborization using three different approaches; rat cortical neurons incubated with the tyrosine kinase inhibitor K252a (Tapley et al., 1992), cortical neurons derived from $TrkB^{F616A}$ knock-in mice (Chen et al., 2005), and cortical neurons derived from p75 $KO^{exonIII}$ mice (Lee et al., 1992). To evaluate morphological changes in neurons, we transfected compartmentalized cultures of cortical neurons (6 DIV) with plasmids driving the expression of EGFP, and then we performed MAP2 immunostaining after neuronal fixation (Fig.1A). To identify the neurons that projected their axons to the axonal compartment (AC), we used the subunit B of the cholera toxin that is fluorescently labeled (Ctb). Ctb is internalized and retrogradely transported in neuronal axons and accumulates in the Golgi apparatus in neuronal cell bodies (Escudero et al, 2019) (Fig. 1A and Supplementary Fig. 1A). The axonal treatment of Ctb allows us to control the true compartmentalization of the microfluidic chambers. Indeed, just cultures that show Ctb accumulation in the Golgi apparatus in the cell body of neurons and not all over the neurons were considered for analysis (Supplementary Fig. 1B). Also, quantifications were performed just in neurons that were labeled by Ctb. Since BDNF is also released from dendrites (Matsuda et al., 2009), the selectivity of BDNF axonal stimulation was

achieved by incubating with the TrkB-Fc chimera protein the neuronal somas in the cell body compartment (CB) (Shelton et al., 1995). TrkB-Fc neutralizes the activity of endogenous BDNF released by neurons; indeed, when TrkB-Fc was not included in the CB compartment, there was an increase in the basal level of dendritic arborization (Supplementary Fig.1C).

Following the above-mentioned experimental design, we found that BDNF added to axons was able to increase primary dendrites, branching points and the overall dendritic arbor in the cell body of rat (Fig. 1C-F) or mice (Fig. 1G-J) cortical neurons. Also, we found that this effect required axonal TrkB signaling. The treatment of rat cortical cultures with K252A in axons abolished the axonal BDNF effect (Fig. 1C-F). Consistently, the treatment of axons with 1NM-PP1 of compartmentalized neuronal cortical cultures derived from $TrkB^{F616A}$ knockin mice abolished the axonal BDNF effect in neuronal morphology (Fig. 1G-J) in the same line with the results observed with K252A in rat-derived cortical cultures.

To evaluate the contribution of p75 to the dendritic arborization induced by BDNF, we used cortical neurons derived from p75 $KO^{exonIII}$ mice. Using the same experimental design described for Figure 1A, we prepared cultures derived from p75 $KO^{exonIII}$ ($p75^{+/+}$), heterozygous ($p75^{+/-}$), and homozygous p75 $KO^{exonIII}$ ($p75^{-/-}$) mice. We observed that the number of branching points induced by axonal stimulation with BDNF was unchanged by the p75 genotype (Fig. 2A-C). However, we found that the absence of p75 changes the basal morphology of the dendritic arbor. While neurons possessed a smaller number of primary dendrites, there was an increased number of distal dendrites (Fig. 2D). Consistently, with the result presented in Fig 2A-C, axonal BDNF was able to increase the number of primary dendrites in p75 $KO^{exonIII}$ to similar levels compared to neurons derived from $p75^{+/+}$ littermates derived from p75 $KO^{exonIII}$ heterozygotes (Fig.2E). Altogether, these results

indicate that BDNF in axons of cortical neurons increases the dendritic arbor in a TrkB activity dependent-manner.

CREB activity is required for BDNF long-distance signaling.

Several groups have shown that axonal BDNF signaling promotes nuclear CREB phosphorylation in different neuronal models (Deinhardt et al., 2006; Watson et al., 1999; Zhou et al., 2012); however, the physiological relevance of CREB activation in this process has not been evaluated. To evaluate CREB activation, we used a well-described polyclonal antibody against phosphorylated CREB at serine 133 (Lonze et al, 2002; Gonzales et al, 2019) and we performed a time course of CREB phosphorylation induced by axonal BDNF treatment. With this aim, at 5 DIV, we incubated Ctb555 in the axonal compartment overnight, to identify all the neurons that projected their axons. At 6 DIV, we added BDNF together with Ctb647 at different time points to parallel bulk retrograde transport with the visualization of CREB phosphorylation (Fig. 3A). BDNF induced an increase of nuclear CREB phosphorylation as soon as 30 minutes, with two peaks, one at 30 and a second peak at 180 minutes. Although Ctb647 accumulation was observed at early times points of BDNF treatment, we found a robust increase of Ctb647 in cell bodies at 180 minutes (Fig. 3B and C).

To corroborate that CREB activity was required for dendritic arborization, we stimulated axons with BDNF of cortical neurons incubated with KG501 in the cell body compartment for 48 hours. KG501 is a small molecule that disrupts the interaction between CREB and the CREB binding protein (CBP) (Best et al., 2004), (Fig. 3D). Interestingly, the presence of KG501 produces a small decrease, but not statistically significant, of the basal dendritic arborization (Fig. 3F). However, KG501 abolished the increase of dendritic arborization induced by the treatment of axons with BDNF (Fig. 3E, F, G, and H). Besides, we evaluated whether p75 was required for phosphorylation

of CREB upon BDNF stimulation. Consistently with the results observed in Fig. 2, the absence of p75 did not impact in BDNF-induced CREB phosphorylation (Fig. Supplementary 2 A and B). Indicating that, in our model, p75 is not required for BDNF-induced CREB phosphorylation.

Since CREB has been widely described as a significant regulator of neurotrophins-induced survival in PNS neurons (Bonni et al., 1999; Lonze and Ginty, 2002), we assessed whether, in our conditions, KG501 had any effect on neuronal survival using the Tunel assay. We found that after 48 hours of treatment, KG501 did not affect neuronal survival. As a positive control, we used oligomycin A, an inhibitor of oxidative phosphorylation in the mitochondria, that induces apoptotic cell death (Fig. 3I and J). Our result suggests that axonal BDNF promotes CREB phosphorylation and that CREB-dependent transcription is required for long-distance dendritic branching induced by BDNF.

Dynein dependent transport of endocytosed TrkB in axons is required for BDNF long-distance signaling.

In axons, long-range retrograde transport of organelles and signaling molecules is performed by the minus-end microtubule molecular motor dynein (Hirokawa et al., 2010). Several groups have shown that in central neurons, BDNF and TrkB are efficiently retrogradely transported (Olenick et al., 2019; Zhou et al., 2012). To further confirm that this process is dynein dependent, we monobiotinylated BDNF *in vitro,* and we labeled it with streptavidin quantum-dots (QD) for *in vivo* imaging (Stuardo et al, 2010). We found that BDNF-QD was efficiently targeted to the retrograde transport pathway and that this process was reduced in about 80% by inhibition of dynein with Ciliobrevin D (CilioD), a specific inhibitor of dynein ATP activity (Sainath and Gallo, 2015) (Fig. 4A and B). To evaluate whether axonal dynein inhibition reduced the transport of axonal TrkB signaling, we evaluated nuclear phosphorylation of CREB and dendritic arborization

induced by axonal BDNF stimulation in the presence or absence of CilioD in axons (Fig 4C). First, we evaluated the extent of CREB phosphorylation in the nucleus upon axonal BDNF stimulation. With this aim, we incubated the axonal compartment overnight with Ctb555 to identify all the neurons that projected their axons, then the next day, we produced the axonal compartment with BDNF and Ctb647 in the presence or absence of CilioD (Fig. 4C and D). The presence of CilioD in the axons decreased CREB phosphorylation at 30 minutes in almost a 40% (Fig. 4D and E) and 180 minutes abolish CREB phosphorylation (Fig. 4D and F) induced by BDNF axonal stimulation in addition to the accumulation of Ctb647 (in magenta) (Fig. 4D). Consistently with the result presented in Fig. 3, reduced CREB phosphorylation induced by dynein inhibition (48 hrs treatment) negatively regulated dendritic arborization caused by axonal BDNF (Fig. 4G - J).

Several lines of research have suggested that signaling endosomes requires a Rab5-dependent sorting step for retrograde transport of neurotrophin receptors (Deinhardt et al, 2006; Escudero et al, 2019; Goto-Silva et al, 2019). Consistently, we observed that endocytosed TrkB co-localized with endogenous Rab5 by using cortical neurons in microfluidic devices (Supplementary figure 3A). In this experiment, we transfected neurons with a plasmid driving the expression of TrkB NH2-tagged with the Flag epitope (Flag-TrkB), and we incubated the distal axons with a Flag-specific monoclonal antibody in the presence of BDNF for 30 or 180 minutes. Then, we evaluated if the Flag staining colocalized with endogenous Rab5 endosomes using a specific antibody against Rab5. We observed that 30 minutes of BDNF treatment was not enough to find an extensive accumulation of Flag-TrkB in the microgrooves required to analyzed co-localization. Therefore, we performed longer time exposure with BDNF (180 min), and we analyzed the TrkB and Rab5 co-localization in axons in the axonal compartment as well as in the microgrooves, were TrkB staining corresponded to retrogradely transported TrkB receptor (Supplementary fig. 3A and B).

Interestingly, we observed that in the axonal compartment, 60% of Flag-TrkB dots colocalized with Rab5 positive vesicles. This colocalization decrease to 40% in the microgrooves (Supplementary fig. 3A and B), suggesting that during its transport, TrkB-positive endosomes mature to another type of endosomes.

The active form of Rab5 recruits different adaptors allowing early endosomes to interact with molecular motors such as dynein and myosins, or SNAREs proteins allowing the fusion of vesicles and endosomal kinases enabling the synthesis of phosphatidylinositols (Christoforidis et al., 1999; Olenick et al., 2019; Wandinger-Ness and Zerial, 2014; Satoh et al, 2008). Previously, we have shown that BDNF promotes Rab5 activation in dendrites and cell bodies of hippocampal neurons (Moya-Alvarado et al., 2018). We used the glutathione-S-transferase (GST)-fused Rab5 binding domain of Rabaptin5 (Rab5BD-GST) to assesses whether, in axons, BDNF also promotes the activation of Rab5 in compartmentalized cortical neurons. This protein recognizes the GTP-bound active form of Rab5 (Wu et al., 2014), and by using an antibody against GST, we have measured the Rab5-GTP levels *in situ* by immunofluorescence (Moya-Alvarado et al, 2018). With the same methodology, we found that the treatment of the axonal compartment of cortical neurons with BDNF for 30 minutes increased the amount of Rab5-GTP in the axons (Supplementary fig. 3C and D). To corroborate that the activation of Rab5 is TrkB specific, we incubated the axonal compartment with K252a or Ctb. We observe that K252a abolished BDNF-induced Rab5 activation, and the addition of Ctb did not increase Rab5 activity (Supplementary fig. 3C and D), both results suggest that BDNF specifically increases the Rab5 activity in a TrkB-dependent manner in axons.

The somatodendritic activity of axonal TrkB is required for long-distance signaling triggered by BDNF in axons.

Several articles have shown that BDNF in axons is processively transported in the retrograde direction accumulating in cell bodies (Olenick et al., 2019; Zhou et al., 2012; Xie et al, 2012). These results, together with the observations presented in this research, suggested that BDNF is transported along with TrkB in signaling endosomes to the cell body where the complex continues signaling.

To our knowledge, there is no evidence that active TrkB reaches the cell body and continues signaling to allow CREB activation. We and others have shown that CREB activation requires Erk1/2 signaling (Finkbeiner et al, 1997; Gonzalez et al, 2019); therefore, it is possible that active Erk in the axons is transported in a complex with dynein and not in signaling endosomes together with active TrkB. Such a mechanism has been described before in the PNS for axonal-injury signals (Perlson et al, 2005). To achieve this aim, we used compartmentalized cultures derived from the $TrkB^{F616A}$ knock-in mice to activate TrkB receptors by BDNF in the axonal compartment and two inhibit their activity upon their arrival to the cell bodies by treating the cell body compartment with 1NM-PP1. For this experiment to work, the $TrkB^{F616A}$ inhibitor NM-PP1 has to be able to reduce TrkB activity after BDNF has activate the receptor. To characterize whether 1NM-PP1 turned off TrkB signaling after BDNF activation, we stimulated the neurons with BDNF for 30 minutes, and then, we incubated with 1NM-PP1 or DMSO for an additional 30 minutes. As a control, we preincubated the neurons with 1NM-PP1 for 1 hour to prevent the activation of TrkB (Fig.5A), as expected the preincubation of neurons with 1NM-PP1 prevented the activation of TrkB and Akt. In addition, we observed that the treatment with 1NM-PP1 after BDNF stimulation decreased the phosphorylation of TrkB and Akt by Western blot to similar basal levels compared to the pre-incubation (Fig.5B, C and D). Consistently, by immunofluorescence, we observed that this treatment reduces the nuclear phosphorylation of CREB and the phosphorylation of 4E-BP1

and 6S ribosomal protein (S6r), two proteins downstream of TORC1 activation induced by BDNF (Fig 5D, E, F, G and H). These results indicate that 1NM-PP1 can turn off the TrkB receptor after its activation and that the TrkB receptor activity is required to sustain TrkB-signaling pathways.

To evaluate whether axonal-derived active TrkB is required for the propagation to cell bodies of BDNF axonal signaling, we first performed a pulse and chase experiment to visualize active TrkB in endosomes and then reduced the activity of TrkB receptors with 1NM-PP1 after their activation with BDNF applied to axons.

We transfected cortical neurons in microfluidic devices with the Flag-TrkB plasmid, and then we treated distal axons with Flag-specific antibody at 4ºC (40 min), washed and treated the axon with or without BDNF for 3 hours at 37ºC. After fixation, we evaluated the co-localization of Flag immunostaining with an antibody against phosphorylated TrkB (pTrkB) in the microgrooves in the proximity to the axonal compartment (distal microgrooves), in the vicinity with the cell bodies compartment (proximal microgrooves) and the cell body compartment (CB) (Supplementary Fig. 4A´and A´´). In the distal microgrooves, we observed that the Flag-TrkB protein is retrogradely transported in the absence of stimulation, but BDNF increases its retrograde transport (Supplementary Fig. 4B). In the proximal microgrooves, little Flag labeling is observed in the absence of axonal BDNF, but there is extensive labeling for Flag-TrkB in the presence of axonal BDNF. There, some vesicles co-localized with both pTrkB and Flag-TrkB (Supplementary Fig. 4C). The colocalization of pTrkB with Flag-TrkB was even more evident in the proximity to the somas (Fig. 6 A and B). These results suggest that axonal BDNF induces the retrograde transport of TrkB and that retrogradely transported TrkB is active in neuronal cell bodies.

Subsequently, we directly tested whether we could reduce the TrkB activity in the cell body after the axonal stimulation of BDNF in TrkB^{F616A} mice-derived neurons. Somatodendritic TrkB activity was tested after treating with 1NM-PP1 in the cell body compartment or in the axonal compartment (Fig. 6C). BDNF applied in the axonal compartment increases the immunostaining for endogenous phosphorylated TrkB in the cell body compartment (Fig. 6D and E). Consistently with the observations in non-compartmentalized neuronal cultures, the presence of 1NM-PP1 in the axonal compartment completely abolished the accumulation of phosphorylated TrkB in cell bodies (Fig. 6D and E). On the other hand, the presence of 1NM-PP1 in the cell body decreased the amount of active TrkB in cell bodies after axonal stimulation with BDNF (Fig. 6D and E). These results suggest that 1NM-PP1 turned off the phosphorylation of endosomal TrkB after arriving at the cell body. To further corroborate this possibility, we studied the phosphorylation of CREB after the stimulation of axons with BDNF in the presence or absence of 1NM-PP1 in cell bodies of compartmentalized cultures derived from TrkB^{F616A} mice. We found that somatodendritic TrkB activity was required for CREB phosphorylation induced by axonal BDNF stimulation (Fig. 6F and G). Altogether, our finding indicates that signaling endosomes carrying active TrkB are required for the propagation of BDNF axonal signaling up to the nucleus of central neurons.

Somatodendritic PI3K/Akt/mTOR activity is required for dendritic branching induced by axonal BDNF.

BDNF-mediated dendritic arborization is achieved by activating the PI3K/Akt/mTOR signaling pathway increasing local translation (Dijkhuizen and Ghosh, 2005; Kumar et al., 2005). Also, PI3K has been shown to mediated retrograde NGF-signaling in sympathetic neurons (Kuruvilla et al., 2000). On the other hand, it was reported that Rab5/APPL1 endosomes were positive for TrkB

and Akt (Goto-Silva et al., 2019), suggesting that axonal PI3K/Akt signaling may contribute to long-distance dendritic arborization induced by BDNF. With this aim, we incubated the axonal compartment of compartmentalized cortical neurons with BDNF in the presence or absence of LY294002, a potent general PI3K inhibitor (Fig. 7A). However, the presence of LY294002 in axons did not affect the dendritic arborization induced by axonal BDNF (Fig. 7B-E). Confirming previous results (Finsterwald et al; 2010), LY294002 was able to reduce BDNF-induce dendritic arborization in non-compartmentalized cortical cultures, indicating that LY294002 was active in cortical neurons (Supplementary fig. 5). Also, inhibition of PI3K activity in the axons did not reduce the transport of BDNF-QD (Fig. 7F and G). This result indicates that PI3K action is not required for retrograde transport of BDNF axonal signaling. Therefore, we investigated whether PI3K signaling in the somatodendritic compartment was required for axonal BDNF-induced dendritic arborization by treating the cell body compartment of compartmentalized cortical cultures with LY294002 (Fig. 7H). We observed that the presence of LY294002 in the CB inhibited the dendritic arborization induced by BDNF (Fig. 7I-L), suggesting that PI3K activation in cell bodies is required for long-distance signaling induced by BDNF in axons.

Once PI3K is activated, it phosphorylates PIP2 two PIP3 in membranes leading to the recruitment of Akt and its phosphorylation by PKD. In turn, Akt activates the mTOR kinase pathway by reducing the activity of the Rheb GAP, leading to the activation of mTOR (Garza-Lombo and Gonsebatt, 2016). First, to evaluate the activation of the mTOR pathway by BDNF in cortical neurons we stimulated non-compartmentalized cultures with BDNF during 1 hour in the presence or absence of LY294002 (PI3K inhibitor), and Torin1, a specific inhibitor of mTOR that will reduce the activity of both the TORC1 and TORC2 complex (Liu et al., 2010). We observed by Western blot that BDNF promotes the phosphorylation of TrkB, Akt, S6r, and 4E-BP1 in

cortical neurons and that the presence of LY294002 and Torin1 fully inhibit the phosphorylation of Akt, S6r and 4E-BP1 but not TrkB (Supplementary figure 5C) as expected. Then, we evaluated whether the mTOR pathway is involved in increasing local translation of protein upon arrival of pTrkB signaling endosomes to cell bodies. With this aim, using rat compartmentalized cortical neurons, we evaluated in the neuronal cell bodies the time course of 4E-BP1 phosphorylation induced by axonal BDNF stimulation. We observed that BDNF increases the phosphorylation of 4E-BP1 at 90 minutes with the higher level at 180 minutes (Fig. 8A and B), and similar results were obtained with the phosphorylation of the S6r (Supplementary fig. 5D and E). To evaluate whether the activation of 4E-BP1 and S6r by axonal BDNF was dependent on the somatodendritic activity of PI3K and mTOR, we treated compartmentalized neurons with the LY294002 or Torin1 inhibitors in the cell body compartment (Fig. 8C). The somatodendritic 4E-BP1 phosphorylation induced by axonal BDNF was significantly reduced by the presence of these inhibitors (Fig. 8D and E). Also, the treatment of axons with the dynein inhibitor CilioD reduced the somatodendritic 4E-BP1 phosphorylation induced by axonal BDNF (Fig. 8D and E). Altogether, these results indicate that BDNF/TrkB signaling endosome activates PI3K/Akt/mTOR pathway in cell bodies suggesting that upon arrival to cell bodies, signaling endosomes turns on protein translation.

CREB and mTOR activities are required for protein synthesis in the somatodendritic compartment.

The results presented above, indicating that BDNF in axons activates the phosphorylation of CREB (Fig. 3) and the activation of mTOR (Fig. 8), suggested that BDNF/TrkB signaling endosome activates the translation of newly synthesized transcripts. To test this hypothesis, we used the metabolic labeling of newly synthesized protein using the click-IT chemistry that uses the incorporation of AHA. AHA is a modified amino acid that resembles methionine (Dieterich et al.,

2010). In addition, to evaluate by immunofluorescence the level of *de novo* protein synthesis, we assessed the levels of Arc, an immediate-early gene, whose protein is required for synaptic plasticity induced by BDNF (Ying et al., 2002) and its synthesis is regulated by CREB and mTOR (Takei et al., 2004; Ying et al., 2002). First, we standardized the click-IT AHA methodology, in non-compartmentalized neurons by stimulating the neurons with BDNF during 5 hours in the presence or absence of cycloheximide. As we expected, BDNF increased the AHA fluorescence, and the presence of cycloheximide significantly reduced the fluorescence of AHA (Supplementary fig 6). Using compartmentalized cultures, we depleted the neurons media of methionine and B27 for 1 hour. Next, we added AHA reagent in all the chamber and BDNF exclusively in the axonal compartment for 5 hours in the presence or absence of KG501 or Torin1 in the cell body compartment (Fig. 9A). As shown in Figure 9, BDNF causes a significant increase of both AHA incorporation in newly synthesized proteins and Arc levels in the cell body and dendrites (Fig. 9B-D). Remarkably, inhibition of CREB and mTOR resulted in a significant reduction in the AHA incorporation in newly synthesized proteins and Arc protein levels in the cell body induced by BDNF (Fig. 9B-D). Altogether, these results indicate that BDNF/TrkB long-distance signaling turns on transcription and translation of specific mRNAs, and signaling endosomes have a role in coordinating both processes.

DISCUSSION

Long-distance communication of neurotrophins is well-described in the PNS, where targeted derived-neurotrophins control survival and axonal growth of sympathetic neurons (Harrington and Ginty, 2013; Ye et al., 2003; Cosker and Segal, 2014; Scott-Solomon and Kuruvilla, 2018; Escudero et al, 2019). Whether long-distance signaling has a role in the physiology of the CNS in mammals is poorly understood. We showed that BDNF in axons could increase dendritic arborization in cell bodies in a TrkB-dependent manner using compartmentalized cultures of cortical neurons. Axonal BDNF increased nuclear CREB activation and translation of newly synthesized proteins in a CREB and PI3K-mTOR dependent-manner. Interestingly, PI3 kinase activity was not required in the axons for long-distance responses, contrary to the observation in sympathetic axons about NGF transport and signaling (Kuruvilla et al., 2000). We also provide evidence indicating that active TrkB, in signaling endosomes, is responsible for axon to cell body responses. BDNF added to axons increased the colocalization of TrkB with Rab5 endosomes and increased Rab5 activity, suggesting that internalization through the early endosomal pathway is a sorting step for retrograde transport.

The propagation of neurotrophin signaling in neurons is a complex process because of the polarized morphology of neurons. Most neurons have long axons that can extend centimeters in the brain and spinal cord or even meters in the peripheral nervous system. TrkB receptors are

localized in dendrites and axons in the plasma membrane and intracellular vesicles throughout development (Gomes et al., 2006). On the other hand, BDNF is secreted in an autocrine and paracrine manner by the regulated-secretory pathway in the somatodendritic compartment and dense-core vesicles in axons (Matsuda et al., 2009; Lo et al, 2011). Thus, neurons have to integrate both the local and long-distance neurotrophin signals. Examples of local responses were described by Horch and Kats, where they showed that BDNF released from single-cell promotes dendritic growth in neighboring neurons (Horch and Katz, 2002).

On the other hand, BDNF long-distance effects were described for the retinal ganglion cells (RGC) of *Xenopus* tadpoles, where long-distance BDNF stimulation enhances RGC dendritic arborization, while local BDNF reduces it (Du and Poo, 2004; Lom et al., 2002). Furthermore, previous work in mammal cells has shown that endosomal signaling of BDNF/TrkB is required for dendritic branching in mammal neurons (Zheng et al., 2008, Zhou et al, 2012). All these results supported the idea that long-distance signaling mediated by signaling endosomes regulates dendritic arborization in mammalian cells.

Since BDNF is secreted in an autocrine manner, and TrkB is located in axons and dendrites, the experimental design performed in our study allowed us to distinguish between axonal BDNF signaling and signaling initiated in cell bodies and dendrites. The microfluidic devices used to perform the compartmentalized cultures possess two chambers separated by 400 long microgrooves to allow fluidic isolation (Gluska et al, 2016). The cell body compartment (CB) was kept with a larger volume compared to the axonal compartment (AC) in most of the experiments. Besides, we incubated the CB with TrkB-Fc to capture all the somatodendritic released of BDNF. Moreover, only the dendritic morphology of neurons that projected their axons in the AC was included in the analysis, allowing us to study BDNF axonal signaling selectively. Thus, our results

are the first to clearly demonstrate that BDNF signaling initiated in axons is able to increase dendritic arborization in cell bodies.

Since BDNF can bind p75 and TrkB, we ought to analyze whether long-distance signaling was dependent on TrkB signaling and the requirement for p75 expression in this process. We observed that inhibition of TrkB signaling, using the 1NM-PP1 in compartmentalized cultures derived from $TrkB^{F616A}$ mice showed a reduction in dendritic arborization. Similar results were obtained in compartmentalized cultures of rat cortical neurons treated with the drug K252a in the axons, a drug that reduces tyrosine kinase activity. Altogether, these results demonstrated that the activation of TrkB in axons activity is required for long-distance signaling triggered by BDNF from axons in cortical neurons. Similarly, long-distance signaling by BDNF and NGF also requires axonal signaling of Trks in sensory and sympathetic neurons, respectively. On the other hand, p75 signaling has been reported as having opposing roles compare to Trks signaling since it can induce apoptosis or reduce axonally when binding different ligands and receptors (Ibanez and Simi, 2012; Kraemer et al., 2014). Also, p75 negatively regulates dendrite complexity and spine density in hippocampal neurons (Zagrebelsky et al., 2005). We observed that the absence of p75 produced a decrease of basal dendritic arborization of cortical neurons in microfluidic devices. Still, the presence of BDNF recover the dendritic complexity, and even increase the distal dendritic arbor, over 50 µm from the soma, suggesting that p75 participates in the regulation of dendritic arborization, but is not required for BDNF axonal signaling.

CREB is a transcription factor (TF) that is endogenously expressed by neurons, and signaling pathways activated by neuronal activity activate CREB by increasing its phosphorylation in the nucleus. Then, CREB increases the transcription of early-genes, including other transcription factors such as c-fos, c-jun, and Egr1 (Flavell and Greenberg, 2008; Yap and Greenberg, 2018).

Thus, CREB plays a central role in physiological brain processes such as learning and memory (Finkbeiner et al., 1997; Xing et al., 1998; Lonze and Ginty, 2002). Indeed, mutations in several co-regulators or downstream TFs are associated with genetic diseases leading to autism and cognitive disabilities (Lyu et al, 2016; Zhou et al, 2016; McGirr et al, 2016; Wang et al, 2018). CREB-dependent gene expression is regulated by two different signaling pathways. The first one by increasing the intracellular Ca^{+2} and the activation of CaMKIV and the second depends on activation of the ERK1/2 pathway (Finkbeiner et al., 1997; Minichiello et al., 2002; Redmond et al., 2002). Whether BDNF in axons is able to activate CREB in cell bodies was suggested before in several studies (Deinhardt et al., 2006; Watson et al., 1999; Zhou et al., 2012); however, no studies have addressed the physiological role of CREB activation by axonal BDNF signaling. In this work, we showed that CREB was required for BDNF-induced long-distance dendritic arborization. Also, CREB activation was required to increase general protein synthesis and the protein expression of the early gene *Arc*.

We performed a time-course study of CREB activation after BDNF addition to axons, and we studied its dependence on dynein activity using the inhibitor Ciliobrevin D (Cilio D). We found a sustained activation of CREB after 3 hours of BDNF addition to axons, results that are different from what we have observed in non-compartmentalized cultures of hippocampal neurons. In hippocampal neurons, the addition of BDNF increases CREB phosphorylation after 15 minutes, and by 1 hour of stimulation, CREB phosphorylation is downregulated (Gonzalez et al 2019). Of note, in compartmentalized cortical cultures, we found that CREB activation, after 30 minutes of BDNF addition to axons was reduced by a 40% by axonal treatment with Cilio D. On the other hand, 3 hours of BDNF stimulation, reduced CREB phosphorylation by an 80%, to a similar extent to what BDNF-QD retrograde transport was reduced. It is possible to speculate that there is an

additional component that contributes to the early activation of CREB by axonal BDNF. Unpublished results of our lab have shown that BDNF in axons is able to increase intracellular calcium levels. Long-distance calcium waves have been described after axonal injury in the PNS (Cho et al., 2013). It is possible that there are two components that allow CREB activation by axonal BDNF, fast propagating calcium waves followed by axonal retrograde transport of signaling endosomes. Interestingly, it has been described that both rapid and sustained CREB phosphorylation is required for proper transcriptional regulation (Dolmetsch et al., 2001), suggesting that in neurons, retrograde BDNF-signaling may contribute to sustained CREB phosphorylation for CREB-dependent maintenance of dendritic arborization. However, more studies are required to support this hypothesis.

Upon ligand binding, TrkB receptors are internalized into endosomes that are retrogradely transported to neuronal cell bodies (Xie et al, 2012). Here, we showed that TrkB is active in the somatodendritic compartment, and the activity of the receptor is required in the cell body for CREB phosphorylation. We used the drug 1NM-PP1 in the cell body to specifically decrease TrkB activity. The fact that 1NM-PP1 reduced the activation of an already active TrkB suggested that 1NM-PP1 binds the ATP binding site of the receptor, reducing the tyrosine activity of TrkB without affecting neurotrophin binding (Chen et al, 2005). There are two possibilities that can explain our results. The first one is that TrkB is being phosphorylated and dephosphorylated during its trajectory along the axon. Such a process will allow 1NM-PP1 to bind the ATP binding cassette of the receptor and prevents its phosphorylation. In the second possibility, BDNF retrograde signaling promotes the phosphorylation of somatodendritic TrkB receptors, and this process is required to maintain CREB phosphorylation. In agreement with this last idea, other groups have shown that retrogradely transported TrkA in sympathetic neurons accumulates in the

somatodendritic compartment locally, increasing the phosphorylation of other TrkA receptors in dendrites and cell body (Lehigh et al., 2017; Yamashita et al., 2017).

The Rab monomeric GTPases are the main regulators of the postendocytic trafficking of endocytic receptors. After internalization, tyrosine kinase receptors enter to the early or sorting endosome, whose biology is regulated by Rab5 (Goh and Sorkin, 2013). Independent of the internalization mechanism of receptors, Rab5 tightly regulates the homotypic fusion of endosomes, forming the sorting endosome (Stenmark, 2009). In the early endosome, the receptor is sorted to the recycling pathway, which is regulated by Rab11 or to the late endocytic pathway regulated by Rab7 (Bronfman et al., 2014). We observed that in axons, and in the presence of BDNF, the colocalization of internalized TrkB with Rab5 is about 60% and then in the microgrooves is reduced to almost 40% of TrkB, suggesting that TrkB is internalized in Rab5 positive endosomes and then sorted to endosomes negative for Rab5. These results indicate that endosomal sorting and transport of signaling endosomes is an active process requiring the active modulation of the endosomal and transport machinery, consistently, Erk1/2 signaling has been shown to be required for dynein-dependent transport of BDNF/TrkB positive endosomes in axons (Mitchell et al, 2012). Moreover, we have shown that BDNF/TrkB signaling is able to increase the activity of the Rab11 and Rab5 GTPases in the dendrites of central neurons (Lazo et al 2013; Moya-Alvarado et al 2018). Previously, in motoneurons, it was shown that neurotrophins receptors are retrogradely transported in endocytic organelle together with a fragment of tetanus neurotoxin TeNT H(C). Rab5 is essential for an early step in the sorting of TeNT H(C) but was absent from axonally transported vesicles that were mainly Rab7 positive (Deinhardt et al, 2006). Other authors have found that retrogradely transported TrkB receptors co-localize with AP2-LC3 organelle (Kononenko et al, 2017). These findings suggest that autophagosomes may have a role for retrograde transport of

neurotrophin receptors (Kononenko et al, 2017). In sympathetic neurons, retrograde transport of TrkA was associated with both Rab7-positive multivesicular bodies and Rab11 positive endosomes (Bardford et al, 2018; Mengchen et al, 2018). These observations suggest, that there is a diversity of Trks signaling organelles originating in the axons (Villarroel-Campos et al, 2018).

We found that the PI3K activity in axons does not play a role in retrograde transport of signaling endosomes. The role of PI3K was anticipated due to the role of phosphoinositide accumulation in early endosomes regulating Rab5-Rab7 transition. This is different from the findings in sympathetic neurons for TrkA signaling, where PI3K activity was required (Kuruvilla et al., 2000). Although we found that LY294002 axonal treatment did not reduce BDNF retrograde transport, it still is possible that PI3K is required for signaling endosome function since TrkB promotes Rab5 activation in axons and Rab5-GTP recruits the class I PI3K complex to early endosomes. Owing to, PI3K has a scaffolding protein activity, that it is not inhibited by LY294002 or wortmannin (Bilanges et al, 2019). For example, p110β is a subunit of class I PI3K scaffolding proteins (Hirsch et al, 2009) and its reduction impairs internalization of transferrin receptor and the epidermal growth factor receptor (EGFR). This phenotype is rescued by the overexpression of the kinase-dead p110β subunit (Ciriaolo et al, 2008; Jia et al, 2008). Moreover, the inhibition of PI3K with wortmannin or LY294002 did not affect the proper retrograde transport of EGF receptor to the lysosomal compartment (Chen and Wang, 2000), suggesting that the regulation of TrkB trafficking could be more similar to EGFR transport than TrkA.

On the other hand, the increase in PI3K activity in the cell bodies was required for BDNF long-distance signaling. Indeed, when PI3K activity was reduced in the cell bodies, the increase in

dendritic branching and activation of mTOR downstream pathways was completely abolished, suggesting that kinase activity of PI3K in the cell body is required for BDNF/TrkB signaling (Luikart et al, 2008). On the other hand, PI3K and Akt kinase activation promotes mTOR phosphorylation induced by BDNF. It has been shown that TrkB endocytosis is required for PI3K/Akt signaling in neuronal cells (Zheng et al., 2008). In addition, in other cell models, TORC1 is located in late endosomes where its activity is regulated by insulin signaling through PI3K activity (Flinn et al., 2010; Sancak et al., 2008; Marat et al, 2017). Here, we found that BDNF axonal signaling promotes somatodendritic phosphorylation of 4E-BP1 and S6 ribosomal protein in a dynein dependent manner, suggesting that mTor in cell bodies is activated by signaling endosomes.

Using Click-iT AHA chemistry, we showed that axonal BDNF promotes protein synthesis in the somatodendritic compartment. AHA incorporation is a method for pulse-labeling of newly synthesized proteins that allow examining changes in protein distribution and turnover when coupled with proximity ligation assay (PLA) (Dieck et al., 2015). We observed that BDNF in axons was able to turn on protein synthesis in the cell bodies in a CREB and PI3K/mTOR dependent manner. These results were parallel by an increase in the protein levels of the Arc protein. It is known that the *Arc* mRNA is anterogradely transported to dendrites to be locally synthesized (Steward and Worley, 2002), suggesting that axonal signaling may increase local translation in dendrites. The fact that these effects were also dependent on CREB suggests that CREB-dependent transcript are specifically translated upon signaling endosome arrival to cell bodies.

Our study demonstrates that BDNF axonal signaling promotes an increase in protein synthesis in the somatodendritic compartment by increasing both CREB and mTOR activation in an

endosomal-dependent manner. Consequently, the arrival of active TrkB to the cell body promotes an increase in the dendritic arborization by the upregulation of CREB activity. It is possible that the retrograde transport of long-distance signaling endosome will have an impact of synaptic plasticity since it has been shown in CNS neurons that BDNF in axons induces a long-distance persistent long-term potentiation on dendrites of retinotectal synapsis in *Xenopus* (Kang and Schuman, 1995; Du and Poo, 2004). Consistently, the activation of CREB has a key role in the activity-dependent expression of genes in neurons, playing a central role in learning and memory (Alonso et al., 2002; Egan et al., 2003). Therefore, our results suggest that BDNF signaling has a direct role in online long-distance regulation of synaptic plasticity and neuronal growth.

METHODOLOGY

Primary culture of cortical neurons. Embryonic cortical neurons from rats (embryonic days 17–19) were obtained from the animal facilities of the Pontificia Universidad Catolica de Chile and euthanatized under deep anesthesia according to the bioethical protocols of our institution. The rat or mouse brain cortex was dissected and dissociated into single cells in HBSS (Hank´s Balance Salt Solution; Thermo-Fisher, cat# 14025134). After disaggregation, neurons were resuspended in MEM/Horse Serum (Thermo-Fisher, cat# 16050122) and were seeded on microfluidic chambers at a low density (40-50 x 10^3 cells/chamber) or in mass culture with a density of 25 x 10^3 cells/well in 12 mm coverslips or 1.8 x 10^6 cell/ 60 mm plate. After four h, the culture medium was replaced with neurobasal medium (Thermo-Fisher, cat# 21103049) supplemented with 2% B27 (Life Technologies, cat# 17504044), 1x glutamax (Thermo-Fisher, cat# 35-050-061) and 1x pen/strep (Thermo-Fisher, cat# 15140-122). The proliferation of non-neuronal cells was limited by the use of cytosine arabinoside (0.25 µg/mL AraC; Sigma-Aldrich, cat# C1768) when MEM/HS was replaced to neurobasal (Gonzalez et al, 2019; Taylor et al., 2003).

Microfluidic devices. The molds to prepare the compartmentalized chambers were provided by Prof Eran Perlson from Tel Aviv University (Gluska et al, 2016). The microfluidic chambers were prepared with a syldgard™ 184 silicone elastomer base (Poirot, cat# 4019862), according to the manufacturer's instructions. Two days before performing primary cultures, glass coverslips (25 mm) were incubated with poly-D-lysine (0.1 mg/mL, Corning, cat# 354210). The next day, poly-D-lysine was washed, and a microfluidic chamber with 400 µm microgrooves was placed on the coverslip. Then, inside of the chamber, a solution of laminin (2 µg/mL in water, Invitrogen, cat# 23017015) was added. The same day that the primary culture was performed, the laminin solution

was changed to DMEM/HS media (Dulbecco Minimum Essential Medium supplemented with 10% horse serum, 1x glutamax and 1x antibiotic/antimycotic, Thermo-Fisher, cat# 15240062).

Quantification of dendritic arborization induced by BDNF. Cortical neurons (6 DIV) were transfected with 0.5 ug of the plasmid driving the expression of EGFP (CA, USA) using 0.8 uL of lipofectamine 2000 (Invitrogen, cat#11668-019) in 30 uL of optimem (Thermo-Fisher, cat# 11058021). After 2 hours, the optimem with the plasmids was replaced for neurobasal media supplemented with 2% B27, 1x Glutamax, and 1x pen/Strep for 1 hour. The cell body compartment was incubated with neurobasal medium supplemented with TrkB-Fc (100 ng/mL, B&D system, 688TK) for all treatments. The drugs were incubated in the cell body compartment or axonal compartment as follows. In the cell body compartment; 1NM-PP1 (1 µM, Cayman, cat# 221244-14-0), KG501 (10 µM, Sigma-Aldrich, cat# 70485), LY294002 (10 µM, Calbiochem, cat# 440202). In the axonal compartment: K252a (0.2 µM, Tocris, cat# 1683), 1NM-PP1 (1 µM), LY294002 (10 µM), Ciliobrevin D (20 µM, Calbiochem, cat# 250401). After 1 hour, BDNF (50 ng/mL, Alomone, cat# B-250) was added to the axonal compartment together with the fluorescently labeled subunit B of the cholera toxin (Ctb, one µg/mL, Thermo-Fisher, cat# C34777). After 48 h, neurons were washed with PBS 37 ºC and then fixed with fresh 4 % paraformaldehyde (Sigma-Aldrich, cat# 158127) in PBS (PFA-PBS) at 37ºC for 15 minutes, then the chamber is removed, and the neurons were permeabilized and blocked with 5% BSA (Jackson, cat# 001-000-162) and 0.5% Triton X-100 (Sigma-Aldrich, cat# 234729) in PBS and then incubated with anti-MAP2 (1:500), (Merk-Millipore, cat# AB5622) in incubation solution (3% BSA with 0.1% Triton X-100 in PBS) after washes (3x buffer) neurons were treated with a donkey anti-mouse Alexa 647 (Molecular probes, cat# A-31571), 1:500, in incubation solution and

mounted for fluorescence microscopy visualization using Mowiol 4-88 (Calbiochem, cat# 475904).

Dendritic arborization was analyzed in cortical neurons labeled with Ctb and transfected with EGFP and labeled with MAP2. Primary dendrites, branching points, and Sholl's analysis (Sholl, 1953) were quantified (see below). For visualization, confocal microscopy using a Nikon Eclipse C2 confocal microscope equipped with a digital camera connected to a computer with Software NIS-Elements C was used. Images were acquired using a 60x objective at 1024x1024 pixel resolution along the z-axis each 0,5 µm of whole cells, 5-7 optical slices. Z-stacks were integrated, and the images were segmented to obtain binary images. Ten concentric circles with increasing diameters (5 µm each step) were traced around the cell body, and the number of intersections between dendrites and circles was counted and plotted for each diameter. The analysis was performed using the ImageJ plugin developed by the Anirvan Gosh Laboratory (http://biology.ucsd.edu/labs/ghosh/software). The number of total primary dendrites and branching points of all dendrites was manually counted from the segmented images.

Evaluation of protein phosphorylation by immunofluorescence. Cortical neurons (5-6 DIV) were incubated with Ctb555 (Ctb, 1 µg/mL) overnight. For all treatments, 6-7 DIV cortical neurons were incubated with neurobasal medium supplemented with TrkB-Fc (100 ng/mL) in the cell body compartment. The drugs were incubated in the cell body compartment or axonal compartment as follows. In the cell body compartment; LY294002 (10 µM), Torin 1 (0.25 µM, Tocris, cat# 4247). In the axonal compartment: Ciliobrevin D (20 µM). After 1 hour, BDNF (50 ng/mL) was added to the axonal compartment together with Ctb647 (1 µg/mL, Thermo-Fisher, cat# C34778). After the time point indicated in the figure, samples were fixed with 4 % PFA containing phosphatase inhibitor (1x, Thermo-Fisher, cat# A32957) in PBS for 15 min. Blockage and permeabilization

were done with blocking solution (5% BSA, 0.3% Triton X-100, 1x phosphatase inhibitor in PBS) for 1 hour. The antibodies were incubated overnight (4ºC) in incubation buffer (BSA, 3%, Triton X100, 0.1%, in PBS). The antibodies used were; anti-phospho-CREB, 1:500, (S133, Cell Signaling cat# 9198), anti-phospho-S6 ribosomal protein 1:100 (S235/236, Cell Signaling, cat# 2211S), anti-phospho-4E-BP1, 1:500 (S65, Cell Signaling, cat# 9456S). The secondary antibody used was a donkey anti-rabbit Alexa488 (1:500), Molecular Probes (cat# A-21206), and was incubated for 90 minutes in BSA (3%), Triton X100 (0.1%) in PBS. The samples were incubated with Hoechst 33342 (5 µg/mL, Invitrogen, cat# 62249) for nuclei visualization. The entire neuron was visualized in the cell body compartment with confocal microscopy using a Nikon Eclipse C2 confocal microscope equipped with a digital camera connected to a computer with Software NIS-Elements C. Images were acquired using a 60x objective at 1024x1024 pixel resolution along the z-axis. Five to seven optical sections of 0,5 µm thick were considered from a whole cell.

Neuron cell viability evaluation through TUNEL assay. For the detection of fragmented DNA, 6 DIV cortical neurons were exposed to KG501 (10 µM) in the cell body compartment and Ctb555 (1 µg/mL) in the axonal compartment, during 48 hrs in neurobasal supplemented with B27. As a positive control, Oligomycin A (10 µM, Sigma-Aldrich, cat# 75351) was incubated in the cell body compartment for 5 min. Neurons were washed with PBS and fixed in 4% PFA in PBS for 15 min at room temperature. After that, neuron-attached coverslips were washed in PBS three times for 5 min each. For permeabilization, neurons were placed onto ice-cold citrate/triton solution (0.1% citrate; 0.1% Triton X-100) and kept for 2 min on ice. Then, the coverslips were washed twice to remove the permeabilization solution and incubated with labeling TUNEL mix (Kit for In Situ Cell Death Detection Kit, Fluorescein, Roche cat# 11684795910) for 1h at 37ºC. The samples were incubated with Hoechst (5 µg/mL). TUNEL assay was analyzed by fluorescence

and/or confocal microscopy and total Hoechst nuclear staining as well as TUNEL positive apoptotic nuclei were counted by using the Image J.

Immunoendocytosis of Flag-TrkB in microfluidic chambers to evaluate retrograde transport of TrkB from axons to dendrites. Cortical neurons (5 DIV) were transfected with 0.5 ug of the plasmid Flag-TrkB (gift from Prof. Francis Lee, NYU, USA) using 0.8 uL of lipofectamine 2000 in 30 uL optimen per chamber. After 48 hours, cortical neurons (7 DIV) were incubated at 4ºC for 10 minutes and then treated with an anti-Flag antibody, 1:750 (Sigma-Aldrich, cat#F3040) for 45 minutes only in the axonal compartment at four ºC. After, cortical neurons were washed briefly with warm neurobasal and were incubated with BDNF (50 ng/mL) in the axonal compartment for 180 minutes. Finally, samples were fixed with a 4 % PFA with a phosphatase inhibitor in PBS for 15 min. Blockage and permeabilization were done with blocking solution (5% BSA, 0.3% Triton X-100, 1x phosphatase inhibitor in PBS) for 1 hour. The antibodies anti phosphorylated TrkB Y816 ,1:200, (Sigma-Aldrich, cat# ABN1381) or anti-Rab ,1:250, (Abcam, cat# AB18211) were incubated overnight (4 ºC) in incubation buffer (BSA, 3%, Triton X100, 0.1%, in PBS). The secondary antibody used was a donkey anti-rabbit Alexa488, 1:500, and donkey anti-mouse Alexa555, 1:500, (Invitrogen, cat# A-31570) was incubated for 90 minutes in incubation buffer. We visualized entire neuron in the cell body compartment, and the microgrooves compartment with confocal microscopy using a Nikon Eclipse C2 confocal microscope equipped with a digital camera connected to a computer with Software NIS-Elements C. Images were acquired using a 60x objective at 1024x1024 pixel resolution along the z-axis each 0,5 µm of whole cells, 5-7 optical slices.

Microscopy detection and quantification of active Rab5 in dendrites and cell bodies. The fusion protein Rab5BD-GST (gift from Prof. Vicente Torres, University of Chile, Chile) was

produced in BL21 E. coli, transformed with a pGEX-GST-Rabaptin5 plasmid and stimulated for 4 hours with IPTG (Promega, cat# V3955). The Rab5BD-GST protein was purified from bacteria lysate using glutathione-Sepharose beads (Sigma-Aldrich, cat# GE17-0756-01). For use as a probe, the protein was eluted in a solution of reduced glutathione (Sigma-Aldrich, cat# G4251) (Moya-Alvarado 2018). Seven DIV Neurons were preincubated with K252a (0.2 µM) during 1 hour in the axonal compartment, then, axonal compartment was stimulated with BDNF (50 ng/mL) or Ctb555 (1 µg/mL) for 30 minutes, fixed with 4 % PFA in PBS for 15 minutes, permeabilized and blocked in 3% fish gelatin (Sigma-Aldrich, cat# G704) in incubation buffer (50 mM Tris-Cl, 50 mM NaCl, 5 mM $MgCl_2$, 0.5 mM DTT, 1 mM EDTA, 0.25 M sucrose and 0.2% Triton X-100, pH 7.2) for 45 min. Then, neurons were incubated overnight with ~10 µg/mL Rab5BD-GST in incubation buffer at 4°C. After two brief washes in HBSS, neurons were fixed again with 4% PFA in PBS, then samples were permeabilized and blocked with 3% fish gelatin (Jackson, cat# 001-000-162) and 0.5% Triton X-100 (Sigma-Aldrich, cat# 234729) in PBS and then incubated with anti-GST, 1:500, (Thermo-Fisher, cat# 8-326) and anti- β-III Tubulin, 1:750, (Sigma-Aldrich, Cat T8578) in incubation solution (3% fish gelatin with 0.1% Triton X-100 in PBS), after washes (3x buffer) neurons were treated with donkey anti-rabbit Alexa488, 1:500, and donkey anti-mouse Alexa647, 1:500, in incubation solution and mounted for fluorescence microscopy visualization.

To avoid biases in the selection of a neuron with high or low levels of Rab5BD-GST, neurons were selected according to the β-III tubulin labeling for quantification. We visualized the proximal part to the microgrooves of the axonal compartment with confocal microscopy using a Nikon Eclipse C2 confocal microscope equipped with a digital camera connected to a computer with Software NIS-Elements C. Images were acquired using a 60x objective at 1024x1024 pixel resolution along the z-axis. Three to five optical sections of 0,25 µm thick were considered per

axons, and 30 μm length of axons were quantified for anti-GST fluorescence. The background was calculated from images of neurons treated with GST, and this baseline was calculated for and subtracted from each dataset.

Evaluation of the somatodendritic TrkB activity in compartmentalized cultures using cortical neurons derived from the TrkB^{F616A} mice. Cortical neurons derived from TrkB^{F616A} (6 DIV) mice were incubated in the axonal compartment with Ctb555 (1 μg/mL) overnight. Then, neurons were washed with neurobasal. In the control and BDNF treatments, cultures were depleted of B27 (neurobasal, with 1x glutamax) during 1 hour and next maintained with more volume of media in the CB in the presence of TrkB-Fc (100 ng/mL). The axonal compartment (AC) was treated with BDNF (50 ng/mL) for 3 hrs. For inhibition of TrkB activity in the cell body compartment (CB), the cultures were depleted from media during one hour in the presence of 1NM-PP1 (1 μM) in the CB, but with more media in the AC to avoid the leak of 1NM-PP1 to the AC. Next, neurons were incubated in the presence or absence of BDNF (50 ng/mL) in the AC with more volume in the AC, and the CB compartment continued with 1NM-PP1 (1 μM) and TrkB-Fc (100 ng/mL) for 3 hours. When the activity of TrkB was inhibited in the AC, neurons were depleted from media during one hour in the presence of 1NM-PP1 (1 μM) in the AC. Then cells were incubated with BDNF (50 ng/mL) in the AC in the presence of 1NM-PP1 and TrkB-Fc for 3 hours with more volume in the CB. For all conditions, the CB was incubated during the experiment with TrkB-Fc (100 ng/mL) in neurobasal without B27. After 3 hours of BDNF treatment, neurons were washed with PBS 1X, and cells were fixed with 4 % PFA in PBS for 15 minutes at room temperature. Finally, immunofluorescence against phosphoproteins was performed as described above. Phospho-TrkB (Y816; 1:200) and phosphor-CREB (S133, 1:500) was evaluated. To evaluate phosphor-TrkB and phosphor-CREB levels, we visualized entire neuron in the cell body

compartment with fluorescent microscopy using a Nikon Eclipse C2 confocal microscope equipped with a digital camera connected to a computer with Software NIS-Elements C. Images were acquired using a 60x objective at 1024x1024 pixel resolution along the z-axis of whole cells. Dots associated with Phospho-TrkB levels in the cell body were quantified from Ctb positive cells and normalized to the size of the cell body compartment. Phospho-CREB levels were evaluated as described above.

Evaluation of the TrkB activity and downstream signaling in non-compartmentalized cultures using cortical neurons derived from the TrkB^{F616A} mice. Cortical neurons derived from TrkB^{F616A} **(**7 DIV**)** mice were depleted from media for 1 hour in the presence or absence of 1NM-PP1 (1 μM). Then neurons were treated as follows: control: vehicle 1 hour. BDNF: incubation of BDNF (50 ng/mL) for 30 minutes, next were rinsed twice with PBS 1x and incubated with the vehicle for 30 minutes. 1NM-PP1 (Pre); neurons were incubated with BDNF in the presence of 1NM-PP1 for 1 hour. 1NM-PP1 (Post); neurons were stimulated with BDNF for 30 minutes. Next were rinsed twice with PBS 1x and incubated with 1NM-PP1 for 30 minutes. Next, TrkB and Akt activity were evaluated by western blot and CREB, 4E-BP1 and S6 ribosomal protein (S6r) were evaluated by immunofluorescence. For western blot, cells were lysed with RIPA buffer (0.1 % SDS, 0.5 % NP40, 10 mM Tris-HCl (pH7.5), 1 mM EDTA, 150 mM NaCl, 0.5 % deoxycholic acid) containing protease and phosphatase inhibitors. Standard SDS gel electrophoresis and Western blotting procedures were used to analyze the cell extracts using anti-phosphorylates pTrkB (Y816, 1:1000), TrkB (1:1000, BD bioscience cat#610101). pAkt (S437, 1:1000, Cell signaling cat#9271), Akt (1:1000, Cell signaling cat#9272) and GAPDH (6C5, 1:1000, Santa Cruz cat#sc-32233) antibodies. For immunofluorescence, neurons were washed with PBS 1X, and cells were fixed with 4 % PFA in PBS for 15 minutes at room temperature.

Finally, immunofluorescence against phosphorylated proteins was performed as described above using the following antibodies; anti-phospho-CREB (S133; 1:500), anti-phospho-S6 ribosomal protein (S235/236, 1:100), anti-phospho-4E-BP1 (S65, 1:500) and anti- β-III tubulin (1:750). We visualized the entire neurons in the cell body compartment with confocal microscopy using a Nikon Eclipse C2 confocal microscope equipped with a digital camera connected to a computer with Software NIS-Elements C. Images were acquired using a 20x objective for pCREB and 60x objective for 4E-BP1 and S6r at 1024x1024 pixel resolution along the z-axis of whole cells.

Evaluation of protein synthesis by Click-iT chemistry and Arc immunofluorescence. Compartmentalized cortical neurons (6 DIV) were incubated in the AC with Ctb488 overnight. At 7 DIV neurons were washed with warm PBS 1x, then incubated with DMEM without methionine (Life Technologies, cat# 21013024), supplemented with glutamax 1x and L-cystine (0.201 mM, Sigma-Aldrich, cat#C7602) for 60 minutes. The media was changed to DMEM supplemented with Click-iT AHA (0.1 mM, Thermo-Fisher, Click-iT cat# C10269; AHA cat#C10102) (standardization was done with AHA 0.2 mM, 0.1 mM, 0.05 mM and 0.02 mM), for 5 hours. In addition, the AC of neurons was treated with BDNF (50 ng/mL), and the cell body compartment was incubated with TrkB-Fc (100 ng/mL) and Torin 1 (0.25 µM) or KG501 (10 µM). Neurons were fixed with 4 % PFA in PBS for 15 minutes. Then, the protocol was completed according to the manufacturer's instructions using alkyne Alexa fluor 555 (2.5 µM, Invitrogen, cat# A20013) to conjugate with AHA. Finally, immunofluorescence against Arc (1:300, Abcam, cat# AC118929) was performed as described above for MAP2 immunostaining.

BDNF-avi production and purification. HEK293FT cells were cultured in DMEM, 4.5 g/l glucose, 10% FBS, 1% penicillin/streptomycin. For transfection, HEK293FT cells were grown in 20 plates of 15 cm to ~70% confluency. Cells were changed to 25 ml of DMEM-high glucose

without serum. For transfection, 30 µg of pcDNA3.1-BDNFavi plasmids DNA (gift from Prof. Chengbiao Wu, UCSD, USA) was added to one ml of DMEM-high glucose media, and then 90 µg PEI (45 µL, Polysciences Inc, cat# 23966-1) were added. The mixture was incubated at room temperature for 25 min and was added into the media by the dropwise method. Transfected HEK293FT cells were incubated at 37 ºC, 5% CO_2 for 48 hours post-transfection, and then, the media was collected for protein purification.

Media was harvested and adjusted to 30 mM phosphate buffer, pH 8.0, 500 mM NaCl, 20 mM imidazole (Sigma-Aldrich, cat# I5513), and a cocktail of protease inhibitors (Sigma-Aldrich, cat# P8340). After incubation on ice for 15 min, the media was cleared by centrifugation at 9500 rpm for 45 min using a Hettich 46R centrifuge. Ni-NTA resins (Qiagen) were rinsed twice with the washing buffer (30 mM phosphate buffer, pH 8.0, 500 mM NaCl, 20 mM imidazole, and a cocktail of protease inhibitors). Ni-NTA resins (Qiagen, cat# 30250) were added to the media at a concentration of 0.3 ml Ni-NTA/100 ml media and incubated for 180 minutes at 4ºC. The media/Ni-NTA slurry was loaded onto a column, and the captured Ni-NTA resins were washed with 10 ml wash buffer and eluted with 1 ml elution buffer (30 mM phosphate buffer, pH8.0, 500 mM NaCl, 300 mM imidazole, protease inhibitors). The purity and concentration of BDNF-avi were assessed by Western blot using a standards curve of BDNF (Alomone, cat# B250), and anti-BDNF antibody (1:500, Alomone, cat# ANT-010).

BDNF-avi biotinylation. Purified BDNF-avi was dialyzed with Sanderson water for 15 minutes. BDNF-avi proteinwas biotinylated with an enzymatic reaction using the BirA enzyme. BDNF-avi (600-800 ng) was incubated with biotinylation buffer (50 mM Bicine, 10 mM MGAcO, 50 µM D-Biotin) in the presence of 10 mM ATP and BirA-GST (BirA 1:1 BDNF-avi) during 1 hour at 30ºC with 600 RPM agitation. Then, 10 mM ATP and BirA-GST were added again, and

the incubation was allowed for one additional hour at 30ºC with 600 RPM agitation.

BDNF-bt coupling to streptavidin quantum dots and visualization in microfluidic devices., One µL of QD-655 was added to 10 µL of BDNF-bt (approx. 3 ng/ µL) to allow the binding of BDNF-bt to streptavidin quantum dots -655 (Thermo-Fisher, cat# Q10121MP). Then the BDNF-QD was taken to a final volume of 20 µL with neurobasal media. Then, the mixture was incubated at room temperature in an orbital rocker for 30 minutes. To evaluate the role of PI3K and dynein on BDNF-QD transport in axons, neurons were depleted with neurobasal media during 1 hour in the presence or absence of LY294002 (10 µM) or Ciliobrevin D (20 µM), respectively. Then, the AC was incubated with BDNF-QD (2 nM) in the presence or absence of LY294002 or Ciliobrevin D for 4 hours. Neurons were fixed with 3 % PFA in PBS for 15 minutes at room temperature, washed with PBS, and mounted in mowiol. We visualized the proximal part of the microgrooves to the cell bodies compartment with epifluorescence microscopy using a Nikon Eclipse C2 confocal microscope equipped with a digital camera connected to a computer with Software NIS-Elements C. Three to five optical sections (3-5) of 0,25 µm thick were considered per axons. Images were acquired using a 100x objective at 1024x1024 pixel resolution along the z-axis. The number of BDNF-QD or QD alone were quantified in 90 μm^2 regions of axons located in the microgrooves.

Statistical analysis. The results are expressed as the average ± standard error of the mean (SEM). Sholl's analysis curves were compared with two-way repeated-measures ANOVA, followed by Bonferroni's multiple comparisons. Student's t-test or one-way ANOVA followed by appropriated multiple comparisons test was performed depending on the number of groups used in each experiment. Details about the specific test used, level of significance, and number of replicates are indicated in each figure legends. Statistical analyses were performed using GraphPad

Prism 7 (Scientific Software).

REFERENCES

Alonso, M., Vianna, M.R., Izquierdo, I., and Medina, J.H. (2002). Signaling mechanisms mediating BDNF modulation of memory formation in vivo in the hippocampus. Cell Mol Neurobiol *22*, 663-674.

Barford, K., Keeler, A., McMahon, L., McDaniel, K., Yap, C. C., Deppmann, C. D., and Winckler, B. (2018). Transcytosis of TrkA leads to the diversification of dendritic signaling endosomes. Sci Rep *8*, 4715

Best, J.L., Amezcua, C.A., Mayr, B., Flechner, L., Murawsky, C.M., Emerson, B., Zor, T., Gardner, K.H., and Montminy, M. (2004). Identification of small-molecule antagonists that inhibit an activator: coactivator interaction. Proc Natl Acad Sci U S A *101*, 17622-17627.

Bilanges, B., Posor, Y., and Vanhaesebroeck, B. (2019). PI3K isoforms in cell signaling and vesicle trafficking. Nat Rev Mol Cell Biol. doi: 10.1038/s41580-019-0129-z.

Bonni, A., Brunet, A., West, A.E., Datta, S.R., Takasu, M.A., and Greenberg, M.E. (1999). Cell survival promoted by the Ras-MAPK signaling pathway by transcription-dependent and -independent mechanisms. Science *286*, 1358-1362.

Bronfman, F.C., Lazo, O.M., Flores, C., and Escudero, C.A. (2014). Spatiotemporal intracellular dynamics of neurotrophin and its receptors. Implications for neurotrophin signaling and neuronal function. Handb Exp Pharmacol *220*, 33-65.

Ciraolo, E., Iezzi, M., Marone, R., Marengo, S., Curcio, C., Costa, C., Azzolino, O., Gonella, C., Rubinetto, C., Wu, H., Dastrù, W., Martin, E.L., Silengo, L., Altruda, F., Turco, E., Lanzetti, L., Musiani, P., Rückle, T., Rommel, C., Backer, J.M., Forni, G., Wymann, M.P., and Hirsch, E. (2008). Phosphoinositide 3-kinase p110beta activity: key role in metabolism and mammary gland cancer but not development. Sci Signal *1*, ra3.

Chen, X., Ye, H., Kuruvilla, R., Ramanan, N., Scangos, K.W., Zhang, C., Johnson, N.M., England, P.M., Shokat, K.M., and Ginty, D.D. (2005). A chemical-genetic approach to studying neurotrophin signaling. Neuron *46*, 13-21.

Chen, X., and Wang, Z. (2000). Regulation of intracellular trafficking of the EGF receptor by Rab5 in the absence of phosphatidylinosito 3-kinase activity. EMBO Rep *2*, 68-74.

Cheung, Z.H., Chin, W.H., Chen, Y., Ng, Y.P., and Ip, N.Y. (2007). Cdk5 is involved in BDNF-stimulated dendritic growth in hippocampal neurons. PLoS Biol *5*, e63.

Cho, Y., Sloutsky, R., Naegle, K., and Cavalli, V. (2013). Injury-induced HDAC5 nuclear export is essential for axon regeneration. Cell *155*, 894-908.

Christoforidis, S., McBride, H.M., Burgoyne, R.D., and Zerial, M. (1999). The Rab5 effector EEA1 is a core component of endosome docking. Nature *397*, 621-625.

Cohen, M.S., Bas Orth, C., Kim, H.J., Jeon, N.L., and Jaffrey, S.R. (2011). Neurotrophin-mediated dendrite-to-nucleus signaling revealed by microfluidic compartmentalization of dendrites. Proc Natl Acad Sci U S A *108*, 11246-11251.

Cosker, K.E., and Segal, R.A. (2014). Neuronal signaling through endocytosis. Cold Spring Harb Perspect Biol *6*.

Debaisieux, S., Encheva, V., Chakravarty, P., Snijders, A.P., and Schiavo, G. (2016). Analysis of signaling endosome composition and dynamics using SILAC in embryonic stem cell-derived neurons. Mol Cell Proteomics *15*, 542–557.

Deinhardt, K., Salinas, S., Verastegui, C., Watson, R., Worth, D., Hanrahan, S., Bucci, C., and Schiavo, G. (2006). Rab5 and Rab7 control endocytic sorting along the axonal retrograde transport pathway. Neuron *52*, 293-305.

Dieterich, D.C., Hodas, J.J., Gouzer, G., Shadrin, I.Y., Ngo, J.T., Triller, A., Tirrell, D.A., and Schuman, E.M. (2010). In situ visualization and dynamics of newly synthesized proteins in rat hippocampal neurons. Nat Neurosci *13*, 897-905.

Dijkhuizen, P.A., and Ghosh, A. (2005). BDNF regulates primary dendrite formation in cortical neurons via the PI3-kinase and MAP kinase signaling pathways. J Neurobiol *62*, 278-288.

Dolmetsch, R.E., Pajvani, U., Fife, K., Spotts, J.M., and Greenberg, M.E. (2001). Signaling to the nucleus by an L-type calcium channel-calmodulin complex through the MAP kinase pathway. Science *294*, 333-339.

Du, J.L., and Poo, M.M. (2004). Rapid BDNF-induced retrograde synaptic modification in a developing retinotectal system. Nature *429*, 878-883

Egan, M.F., Kojima, M., Callicott, J.H., Goldberg, T.E., Kolachana, B.S., Bertolino, A., Zaitsev, E., Gold, B., Goldman, D., Dean, M., Lu, B., and Weinberger, D.R. (2003). The BDNF val66met polymorphism affects activity-dependent secretion of BDNF and human memory and hippocampal function. Cell *112*, 257-269.

Escudero, C.A., Cabeza, C., Moya-Alvarado, G., Maloney, M.T., Flores, C.M., Wu, C., Court, F.A., Mobley, W.C., and Bronfman, F.C. (2019). c-Jun N-terminal kinase (JNK)-dependent internalization and Rab5-dependent endocytosis sorting mediate long-distance retrograde neuronal death induced by axonal BDNF-p75 signaling. Sci Rep *9*, 6070.

Finkbeiner, S., Tavazoie, S.F., Maloratsky, A., Jacobs, K.M., Harris, K.M., and Greenberg, M.E. (1997). CREB: a major mediator of neuronal neurotrophin responses. Neuron *19*, 1031-1047.

Finsterwald, C., Fiumelli, H., Cardinaux, J.R., and Martin, J.L. (2010). Regulation of dendritic development by BDNF requires activation of CRTC1 by glutamate. J Biol Chem *285*, 28587-28595.

Flavell, S.W., and Greenberg, M.E. (2008). Signaling mechanisms linking neuronal activity to gene expression and plasticity of the nervous system. Annu. Rev. Neurosci *31*, 563–590.

Flinn, R.J., Yan, Y., Goswami, S., Parker, P.J., and Backer, J.M. (2010). The late endosome is essential for mTORC1 signaling. Mol Biol Cell *21*, 833-841.

Garza-Lombo, C., and Gonsebatt, M.E. (2016). Mammalian Target of Rapamycin: Its Role in Early Neural Development and in Adult and Aged Brain Function. Front Cell Neurosci *10*, 157.

Gluska, S., Chein, M., Rotem, N., Ionescu, A., and Perlson, E. (2016). Tracking quantum-dot labeled neurotrophic factors transport along primary neuronal axons in compartmental microfluidic chambers. Methods cell biol *131*, 365-387.

Goh, L.K., and Sorkin, A. (2013). Endocytosis of receptor tyrosine kinases. Cold Spring Harb Perspect Biol *5*, a017459.

Gomes, R.A., Hampton, C., El-Sabeawy, F., Sabo, S.L., and McAllister, A.K. (2006). The dynamic distribution of TrkB receptors before, during, and after synapse formation between cortical neurons. J Neurosci *26*, 11487-11500.

Gonzalez, A., Moya-Alvarado, G., Gonzalez-Billaut, C., and Bronfman, F.C. (2016). Cellular and molecular mechanisms regulating neuronal growth by brain-derived neurotrophic factor. Cytoskeleton (Hoboken) *73*, 612-628.

Gonzalez, A., Lazo, O.M., and Bronfman, F.C. (2019). The Rab5-Rab11 endosomal pathway is required for BDNF-induced CREB transcriptional regulation in neurons. (Preprint ID#BIORXIV/2019/844720).

Gorski, J.A., Zeller, S.R., Tamowski, S., and Jones, K.R., (2003). Brain-derived neurotrophic factor is required for the maintenance of cortical dendrites. J Neurosci *23*, 6856-6865.

Goto-Silva, L., McShane, M.P., Salinas, S., Kalaidzidis, Y., Schiavo, G., and Zerial, M. (2019). Retrograde transport of Akt by a neuronal Rab5-APPL1 endosome. Sci Rep *9*, 2433.

Grimes, M.L., Zhou, J., Beattie, E.C., Yuen, E.C., Hall, D.E., Valletta, J.S., Topp, K.S., LaVail, J.H., Bunnett, N.W., and Mobley, W.C. (1996). Endocytosis of activated TrkA: evidence that nerve growth factor induces formation of signaling endosomes. J Neurosci *16*, 7950–7964.

Haihong, Y., Kuruvilla, R., Zweifel, L.S., and Ginty, D.D. (2003). Evidence in support of signaling endosome-based retrograde survival of sympathetic neurons. Neuron *39*, 57-68.

Harrington, A.W., and Ginty, D.D. (2013). Long-distance retrograde neurotrophic factor signalling in neurons. Nat Rev Neurosci *14*, 177-187.

Hirokawa, N., Niwa, S., and Tanaka, Y. (2010). Molecular motors in neurons: transport mechanisms and roles in brain function, development, and disease. Neuron *68*, 610-638.

Hirsch, E., Braccini, L., Ciraolo, E., Morello, F., and Perino, A. (2009). Twice upon a time: PI3K's secret double life exposed. Trends Biochem. Sci *34*, 244–248.

Horch, H.W., Kruttgen, A., Portbury, S.D., and Katz, L.C. (1999). Destabilization of cortical dendrites and spines by BDNF. Neuron *23*, 353–364.

Horch, H.W., and Katz, L.C. (2002). BDNF release from single cells elicits local dendritic growth in nearby neurons. Nat Neurosci *5*, 1177-1184.

Huang, E.J., and Reichardt, L.F. (2003). Trk receptors: roles in neuronal signal transduction. Annu Rev Biochem *72*, 609-642.

Ibanez, C.F., and Simi, A. (2012). p75 neurotrophin receptor signaling in nervous system injury and degeneration: paradox and opportunity. Trends Neurosci *35*, 431-440.

Jan, Y.N., and Jan, L.Y. (2010). Branching out: mechanisms of dendritic arborization. Nat Rev Neurosci *11*, 316-328.

Jia, S., Liu, Z., Zhang, S., Liu, P., Zhang, L., Lee, S.H., Zhang, J., Signoretti, S., Loda, M., Roberts, T.M., and Zhao, J.J. (2008). Essential roles pf PI(3)K-p110beta in cell growth, metabolism and tumorigenesis. Nature *454*, 776-779.

Kang, H.J., and Schuman, E.M. (1995). Neurotrophin-induced modulation of synaptic transmission in the adult hippocampus. J Physiol Paris *89*, 11-22.

Kononenko, N.L., Classen, G.A., Kuijpers, M., Puchkov, D., Maritzen, T., Tempes, A., Malik, A.R., Skalecka, A., Bera, S., Jaworski, J., and Haucke, V. (2017). Retrograde transport of TrkB-containing autophagosomes via the adaptor AP-2 mediates neuronal complexity and prevents neurodegeneration. Nat Commun *8*, 14819.

Kraemer, B.R., Yoon, S.O., and Carter, B.D. (2014). The biological functions and signaling mechanisms of the p75 neurotrophin receptor. Handb Exp Pharmacol *220*, 121-164.

Kumar, V., Zhang, M.X., Swank, M.W., Kunz, J., and Wu, G.Y. (2005). Regulation of dendritic morphogenesis by Ras-PI3K-Akt-mTOR and Ras-MAPK signaling pathways. J Neurosci *25*, 11288-11299.

Kuruvilla, R., Ye, H., and Ginty, D.D. (2000). Spatially and functionally distinct roles of the PI3-K effector pathway during NGF signaling in sympathetic neurons. Neuron *27*, 499-512.

Lazo, O.M., Gonzalez, A., Ascano, M., Kuruvilla, R., Couve, A., and Bronfman, F.C. (2013). BDNF regulates Rab11-mediated recycling endosome dynamics to induce dendritic branching. J Neurosci *33*, 6112-6122.

Leal, G., Comprido, D., and Duarte, C.B. (2014). BDNF-induced local protein synthesis and synaptic plasticity. Neuropharmacology *76 Pt C*, 639-656.

Lee, K.F., Li, E., Huber, L.J., Landis, S.C., Sharpe, A.H., Chao, M.V., and Jaenisch, R. (1992). Targeted mutation of the gene encoding the low affinity NGF receptor p75 leads to deficits in the peripheral sensory nervous system. Cell *69*, 737-749.

Lehigh, K.M., West, K.M., and Ginty, D.D. (2017). Retrogradely Transported TrkA Endosomes Signal Locally within Dendrites to Maintain Sympathetic Neuron Synapses. Cell Rep *19*, 86-100.

Liu, K., Xing, R., Jian, Y., Gao, Z., Ma, X., Sun, X., Li, Y., Xu, M., Wang, X., Jing, Y., Guo, W., and Yang, C. (2017). WDR91 is a Rab7 effector required for neuronal development. J Cell Biol *216*, 3307-3321.

Liu, Q., Chang, J.W., Wang, J., Kang, S.A., Thoreen, C.C., Markhard, A., Hur, W., Zhang, J., Sim, T., Sabatini, D.M., and Gray, N.S. (2010). Discovery of 1-(4-(4-propionylpiperazin-1-yl)-3-(trifluoromethyl)phenyl)-9-(quinolin-3-yl)benz o[h][1,6]naphthyridin-2(1H)-one as a highly potent, selective mammalian target of rapamycin (mTOR) inhibitor for the treatment of cancer. J Med Chem *53*, 7146-7155.

Lo, K.Y., Kuzmin, A., Unger, S.M., Petersen, J.D., and Silverman, M.A. (2011). KIF1A is the primary anterograde motor protein required for the axonal transport of dense-core vesicles in cultured hippocampal neurons. Neurosci Lett *491*, 168–173.

Lom, B., Cogen, J., Sanchez, A.L., Vu, T., and Cohen-Cory, S. (2002). Local and target-derived brain-derived neurotrophic factor exert opposing effects on the dendritic arborization of retinal ganglion cells in vivo. J Neurosci *22*, 7639-7649.

Lonze, B.E., and Ginty, D.D. (2002). Function and regulation of CREB family transcription factors in the nervous system. Neuron *35*, 605-623.

Lonze, B.E., Riccio, A., Cohen, S., and Ginty, D.D. (2002). Apoptosis, axonal growth defects, and degeneration of peripheral neurons in mice lacking CREB. Neuron *34*, 371–385.

Luikart, B.W., Zhang, W., Wayman, G.A., Kwon, C.H., Westbrook, G.L., and Parada, L.F. (2008). Neurotrophin-dependent dendritic filopodial motility:A convergence on PI3K signaling. J Neurosci *28*, 7006-7012.

Lyu, J. W., Yuan, B., Cheng, T. L., Qiu, Z. L., and Zhou, W. H. (2016). Reciprocal regulation of autism-related genes MeCP2 and PTEN via microRNAs. Sci. Rep *6*, 20392

Marat, A., Wallroth, A., Lo, W.T., Müller, R., Norata, G.D., Falasca, M., Shultz, C., and Haucke, V. (2017). mTORC1 activity repression by late endosomal phosphatidylinositol 3,4-bisphosphate. Science *356*, 968-972.

Matsuda, N., Lu, H., Fukata, Y., Noritake, J., Gao, H., Mukherjee, S., Nemoto, T., Fukata, M., and Poo, M.M. (2009). Differential activity-dependent secretion of brain-derived neurotrophic factor from axon and dendrite. J Neurosci *29*, 14185-14198.

Mengchen, Y., Lehigh, K.M., and Ginty, D.D. (2018). Multivesicular bodies mediate long-range retrograde NGF-TrkA signaling. eLife *7*, pii:e33012.

Minichiello, L., Calella, A.M., Medina, D.L., Bonhoeffer, T., Klein, R., and Korte, M. (2002). Mechanism of TrkB-mediated hippocampal long-term potentiation. Neuron *36*, 121-137.

Mitchell, D.J., Blasier, K.R., Jeffery, E.D., Ross, M.W., Pullikuth, A.K., Suo, D., Park, J., Smiley, W.R., Lo, K.W., Shabanowitz, J., Deppmann, C.D., Trinidad, J.C., Hunt, D.F., Catling, A.D., and Pfister, K.K. (2012). Trk activation of the ERK1/2 kinase pathway stimulates intermediate chain phosphorylation and recruits cytoplasmic dynein to signaling endosomes for retrograde axonal transport. J Neurosci *32*, 15495-15510.

Moya-Alvarado, G., Gonzalez, A., Stuardo, N., and Bronfman, F.C. (2018). Brain-Derived Neurotrophic Factor (BDNF) Regulates Rab5-Positive Early Endosomes in Hippocampal Neurons to Induce Dendritic Branching. Front Cell Neurosci *12*, 493.

Olenick, M.A., Dominguez, R., and Holzbaur, E.L.F. (2019). Dynein activator Hook1 is required for trafficking of BDNF-signaling endosomes in neurons. J Cell Biol *218*, 220-233.

Perlson, E., Hanz, S., Ben-Yaakov, K., Segal-Ruder, Y., Seger, R., and Fainzilber, M. (2005). Vimentin-dependent spatial translocation of an activated MAP kinase in injured nerve. Neuron 45, 715-726

Ravindran, S., Nalavadi, V.C., and Muddashetty, R.S. (2019). BDNF Induced Translation of Limk1 in Developing Neurons Regulates Dendrite Growth by Fine-Tuning Cofilin1 Activity. Front Mol Neurosci *12*, 64.

Redmond, L., Kashani, A.H., and Ghosh, A. (2002). Calcium regulation of dendritic growth via CaM kinase IV and CREB-mediated transcription. Neuron *34*, 999-1010.

Riccio, A., Pierchala, B.A., Ciarallo, C.L., and Ginty, D.D. (1997). An NGF-TrkA-mediated retrograde signal to transcription factor CREB in sympathetic neurons. Science *277*, 1097–1100.

Sainath, R., and Gallo, G. (2015). The dynein inhibitor Ciliobrevin D inhibits the bidirectional transport of organelles along sensory axons and impairs NGF-mediated regulation of growth cones and axon branches. Dev Neurobiol *75*, 757-777.

Sancak, Y., Peterson, T.R., Shaul, Y.D., Lindquist, R.A., Thoreen, C.C., Bar-Peled, L., and Sabatini, D.M. (2008). The Rag GTPases bind raptor and mediate amino acid signaling to mTORC1. Science *320*, 1496-1501.

Satoh, D., Sato, D., Tsuyama, T., Saito, M., Ohkura, H., Rolls, M. M., Ishikawa, F., and Uemura, T. (2008). Spatial control of branching within dendritic arbors by dynein-dependent transport of

Rab5-endosomes. Nat Cell Biol *10*, 1164–1171.

Schink, K.O., Tan, K.W., and Stenmark, H. (2016). Phosphoinositides in Control of Membrane Dynamics. Annu Rev Cell Dev Biol *32*, 143-171.

Schratt, G.M., Nigh, E.A., Chen, W.G., Hu, L., and Greenberg, M.E. (2004). BDNF regulates the translation of a select group of mRNAs by a mammalian target of rapamycin-phosphatidylinositol 3-kinase-dependent pathway during neuronal development. J Neurosci *24*, 7366-7377.

Scott-Solomon, E., and Kuruvilla, R. (2018). Mechanisms of neurotrophin trafficking via Trk receptors. Mol Cell Neurosci *91*, 25-33.

Shelton, D.L., Sutherland, J., Gripp, J., Camerato, T., Armanini, M.P., Phillips, H.S., Carroll, K., Spencer, S.D., and Levinson, A.D. (1995). Human trks: molecular cloning, tissue distribution, and expression of extracellular domain immunoadhesins. J Neurosci *15*, 477-491.

Shimada, A., Mason, C.A., and Morrison, M.E. (1998). TrkB signaling modulates spine density and morphology independent of dendrite structure in cultured neonatal Purkinje cells. J Neurosci *18*, 8559-8570.

Sholl, D.A. (1953). Dendritic organization in the neurons of the visual and motor cortices of the cat. J Anat *87*, 387-406.

Stenmark, H. (2009). Rab GTPases as coordinators of vesicle traffic. Nat Rev Mol Cell Biol *10*, 513-525.

Steward, O., and Worley, P. (2002). Local synthesis of proteins at synaptic sites on dendrites: role in synaptic plasticity and memory consolidation? Neurobiol Learn Mem *78*, 508-527.

Stuardo N, Moya-Alvarado G, Ramírez C, Schiavo G, Bronfman FC. An Improved Protocol to Purify and Directly Mono-Biotinylate Recombinant BDNF in a Tube for Cellular Trafficking Studies in Neurons. *J Vis Exp*. 2020;(161):10.3791/61262. Published 2020 Jul 11. doi:10.3791/61262

Sutton, M., and Schuman, E.M., (2006). Dendritic protein synthesis, synaptic plasticity, and memory. Cell *127*, 49-58.

Takei, N., Inamura, N., Kawamura, M., Namba, H., Hara, K., Yonezawa, K., and Nawa, H. (2004). Brain-derived neurotrophic factor induces mammalian target of rapamycin-dependent local activation of translation machinery and protein synthesis in neuronal dendrites. J Neurosci *24*, 9760-9769.

Tapley, P., Lamballe, F., and Barbacid, M. (1992). K252a is a selective inhibitor of the tyrosine protein kinase activity of the trk family of oncogenes and neurotrophin receptors. Oncogene *7*, 371-381.

Taylor, A.M., Rhee, S.W., Tu, C.H., Cribbs, D.H., Cotman, C.W., and Jeon, N.L. (2003). Microfluidic Multicompartment Device for Neuroscience Research. Langmuir *19*, 1551-1556.

Terenzio, M., Schiavo, G., and Fainzilber, M. (2017). Compartmentalized signaling in neurons: from cell biology to neuroscience. Neuron *96*, 667–679.

tom Dieck, S., Kochen, L., Hanus, C., Heumuller, M., Bartnik, I., Nassim-Assir, B., Merk, K., Mosler, T., Garg, S., Bunse, S., Tirrel, D.A., and Shuman, E.M. (2015). Direct visualization of newly synthesized target proteins in situ. Nat Methods *12*, 411-414.

Villarroel-Campos, D., Schiavo, G., and Lazo, O. M. (2018). The many disguises of the signalling endosome. FEBS letters *592*, 3615–3632.

Wandinger-Ness, A., and Zerial, M. (2014). Rab proteins and the compartmentalization of the endosomal system. Cold Spring Harb Perspect Biol *6*, a022616.

Wang, H., Xu, J., Lazarovici, P., Quirion, R., and Zheng, W. (2018). cAMP response element-binding protein (CREB): a possible signaling molecule link in the pathophysiology of schizophrenia. Front Mol Neurosci *11*, 255.

Watson, F.L., Heerssen, H.M., Moheban, D.B., Lin, M.Z., Sauvageot, C.M., Bhattacharyya, A., Pomeroy, S.L., and Segal, R.A. (1999). Rapid nuclear responses to target-derived neurotrophins require retrograde transport of ligand-receptor complex. J Neurosci *19*, 7889-7900.

Wong, R.O., and Ghosh, A., (2002). Activity-dependent regulation of dendritic growth and patterning. Nat Rev Neurosci *3*, 803-812.

Wu, K.Y., He, M., Hou, Q.Q., Sheng, A.L., Yuan, L., Liu, F., Liu, W.W., Li, G., Jiang, X.Y., and Luo, Z.G. (2014). Semaphorin 3A activates the guanosine triphosphatase Rab5 to promote growth cone collapse and organize callosal axon projections. Sci Signal *7*, ra81.

Xie, W., Zhang, K., and Cui, B. (2012). Functional characterization and axonal transport of quantum dot labeled BDNF. Integr Biol (Camb) *4*, 953-960.

Xing, J., Kornhauser, J.M., Xia, Z., Thiele, E.A., and Greenberg, M.E. (1998). Nerve growth factor activates extracellular signal-regulated kinase and p38 mitogen-activated protein kinase pathways to stimulate CREB serine 133 phosphorylation. Mol Cell Biol *18*, 1946-1955.

Xu, B., Zang, K., Ruff, N.L., Zhang, Y.A., McConnell, S.K., Stryker, M.P., and Reichardt, L.F. (2000). Cortical degeneration in the absence of neurotrophin signaling: dendritic retraction and neuronal loss after removal of the receptor TrkB. Neuron *26*, 233-245.

Yamashita, N., Joshi, R., Zhang, S., Zhang, Z.Y., and Kuruvilla, R. (2017). Phospho-Regulation of Soma-to-Axon Transcytosis of Neurotrophin Receptors. Dev Cell *42*, 626-639 e625.

Yan, Q., Rosenfeld, R.D., Matheson, C.R., Hawkins, N., Lopez, O.T., Bennett, L., and Welcher, A.A. (1997). Expression of brain-derived neurotrophic factor protein in the adult rat central nervous system. Neuroscience *78*, 431-448.

Yap, E.L., and Greenberg, M.E. (2018). Activity-regulated transcription: Bridging the gap between neural activity and behavior. Neuron *100*, 330-348.

Ye, H., Kuruvilla, R., Zweifel, L.S., and Ginty, D.D. (2003). Evidence in support of signaling endosome-based retrograde survival of sympathetic neurons. Neuron *39*, 57-68.

Ying, S.W., Futter, M., Rosenblum, K., Webber, M.J., Hunt, S.P., Bliss, T.V., and Bramham, C.R. (2002). Brain-derived neurotrophic factor induces long-term potentiation in intact adult hippocampus: requirement for ERK activation coupled to CREB and upregulation of Arc synthesis. J Neurosci *22*, 1532-1540.

Zagrebelsky, M., Holz, A., Dechant, G., Barde, Y.A., Bonhoeffer, T., and Korte, M. (2005). The p75 neurotrophin receptor negatively modulates dendrite complexity and spine density in hippocampal neurons. J Neurosci *25*, 9989-9999.

Zheng, J., Shen, W.H., Lu, T.J., Zhou, Y., Chen, Q., Wang, Z., Xiang, T., Zhu, Y.C., Zhang, C., Duan, S., and Xiong, Z.Q. (2008). Clathrin-dependent endocytosis is required for TrkB-dependent Akt-mediated neuronal protection and dendritic growth. J Biol Chem *283*, 13280-13288.

Zhou, B., Cai, Q., Xie, Y., and Sheng, Z.H. (2012). Snapin recruits dynein to BDNF-TrkB signaling endosomes for retrograde axonal transport and is essential for dendrite growth of cortical neurons. Cell Rep *2*, 42-51.

Zhou, P., Porcionatto, M., Pilapil, M., Chen, Y., Choi, Y., Tolias, K.F., Bikoff, J.B., Hong, E.J., Greenberg, M.E., and Segal, R.A. (2007). Polarized signaling endosomes coordinate BDNF-induced chemotaxis of cerebellar precursors. Neuron *55*, 53-68.

Zhou, W. J., Xu, N., Kong, L., Sun, S. C., Xu, X. F., Jia, M. Z., Wang, Y., and Chen, Z.Y. (2016). The antidepressant roles of Wnt2 and Wnt3 in stress-induced depression-like behaviors. Transl. Psychiatry *6*, e892.

FIGURES

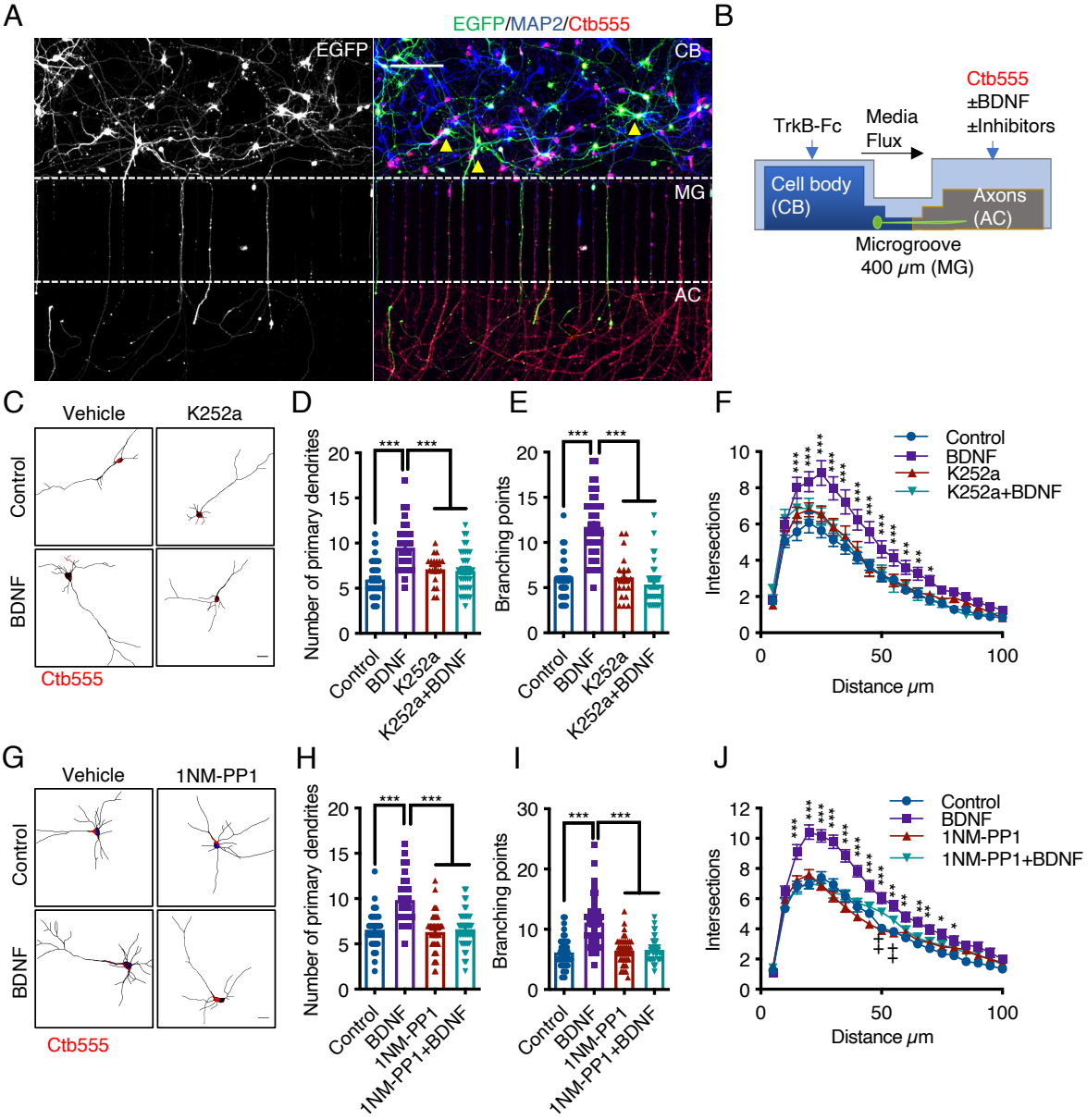
A
EGFP/MAP2/Ctb555
EGFP
CB
MG
AC
B
Ctb555
±BDNF
±Inhibitors
TrkB-Fc
Media
Flux
Cell body
(CB)
Axons
(AC)
Microgroove
400 μm (MG)
C
Vehicle
K252a
Control
BDNF
Ctb555
D
Number of primary dendrites
Control
BDNF
K252a
K252a+BDNF
E
Branching points
F
Intersections
Distance μm
Control
BDNF
K252a
K252a+BDNF
G
Vehicle
1NM-PP1
Control
BDNF
Ctb555
H
Number of primary dendrites
Control
BDNF
1NM-PP1
1NM-PP1+BDNF
I
Branching points
J
Intersections
Distance μm
Control
BDNF
1NM-PP1
1NM-PP1+BDNF

Figure 1. BDNF added to axons promotes dendritic branching in a TrkB-dependent manner. **(A)** Representative images of two compartmentalized microfluidic chambers after BDNF/Ctb555 incubation in the axonal compartment. Cortical neurons were seeded in microfluidic chambers of 400 µm long and 15 µm width microgrooves. Left panel, EGFP immunofluorescence showed in white. Right panel, EGFP in green, MAP2 in blue and Ctb555 in red. Ctb555 in the cell body and co-staining with MAP2 is shown in magenta, in light blue are labelled neurons co-stained with EGFP/MAP2/Ctb555 indicates neurons projecting their axons through the microgrooves (yellow arrow). **(B)** Experimental design to study BDNF retrograde signaling. At Six DIV neurons were transfected with a plasmid driving the expression of EGFP. The cell bodies compartment (CB) was incubated with TrkB-Fc (100 ng/mL). The axonal compartment (AC) was stimulated with BDNF (50 ng/mL) in addition to the fluorescently-labelled B subunit of choleratoxin (Ctb555) in presence or absence of different inhibitors. Treatments with BDNF and TrkB-Fc were performed for 48 hours to evaluate dendritic arborization. Finally, neurons were fixed, and immunofluorescence was performed against MAP2. **(C)** Representative images of rat cortical neurons in the CB (red indicated Ctb555) from compartmentalized cultures treated in the axons with DMSO (control), K252a (200 nM), BDNF (50 ng/mL) or BDNF and preincubated with K252a **(D-F).** Quantification of primary dendrites **(D)**, branching points **(E)** and Sholl analysis **(F)**, from neurons labelled with EGFP/MAP2/Ctb555 for each experimental condition. n= 40-45 neurons from 3 independent experiment. **(G)** Representative images of mouse $TrkB^{F616A}$ cortical neurons in the CB (red indicated Ctb555) from compartmentalized cultures treated in the axons with DMSO (control), 1NM-PP1 (1 µm), BDNF (50 ng/mL), or BDNF pretreated with 1NM-PP1. **(H-J)** Quantification of primary dendrites **(H)**, branching points **(I)** and Sholl analysis **(J)**, from neurons labelled with EGFP/MAP2/Ctb555 in the four different experimental conditions as described in G. Scale bar 20 µm. n= 40-45 neurons from 3 independent experiment. *$p<0.05$, **$p< 0.01$, ***$p< 0.001$, ++$p<0.01$ NM-PP1 vs 1NM-PP1+BDNF. Statistics was done by one-way ANOVA test followed by Bonferroni post-test for multiple comparisons (D, E, H and I). Two-way ANOVA with Bonferroni post-test for multiple comparisons (F and J). Results are expressed as ± SEM.

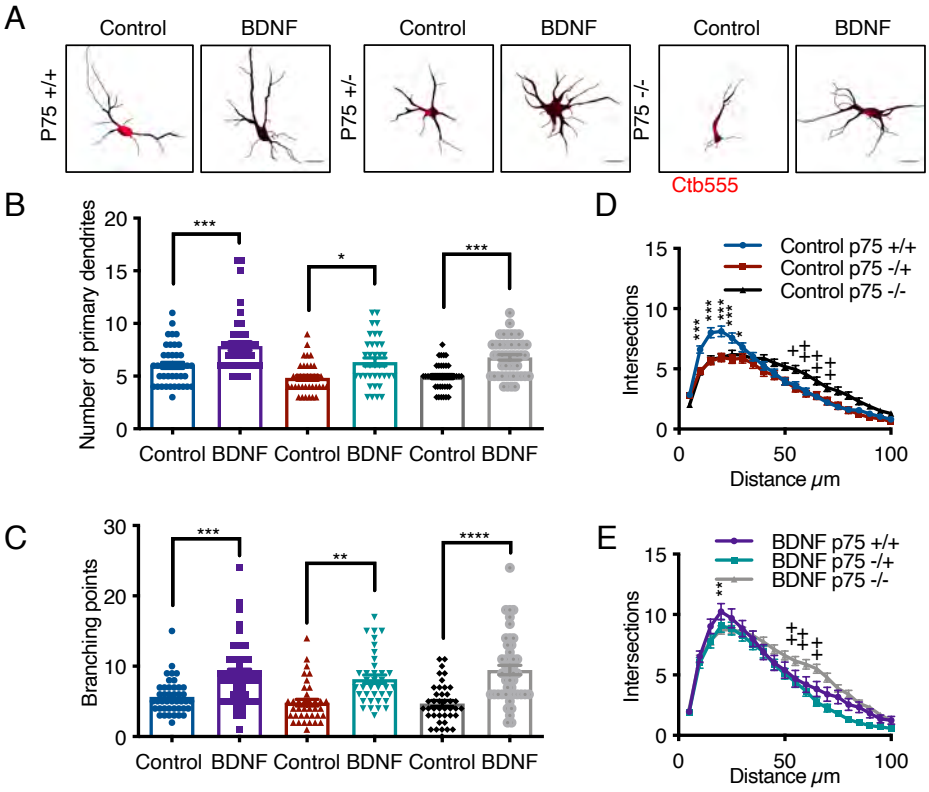

Figure 2. BDNF increases dendritic arborization in a p75-independent manner. (A) Representative images of p75 KO^{exonIII} cortical neurons in the CB (red indicated Ctb555) from compartmentalized cultures of p75$^{+/+}$, p75$^{+/-}$ or p75$^{-/-}$ treated with BDNF (50 ng/mL) in axons. Quantification of primary dendrites **(B)** and branching points **(C)** from neurons labelled with MAP2/Ctb555 in the different mouse genotypes as described in A. **(D)** Sholl analysis of cultures treated with TrkB-Fc in the CB compartment (non-stimulated) condition from each genotype. **(E)** Sholl analysis of cultures treated with TrkB-Fc in the CB compartment and BDNF in the AC from each mouse genotype. n= 40-50 neurons from 3 independent mice, in 2 independent experiments. *p<0.05, **p< 0.01, ***p< 0.001, ++p<0.01 p75$^{-/-}$ vs p75$^{+/+}$. Statistics was done by one-way ANOVA test followed by Bonferroni post-test for multiple comparisons (B and C). Two-way ANOVA with Bonferroni post-test for multiple comparisons (D and E). Results are expressed as ± SEM.

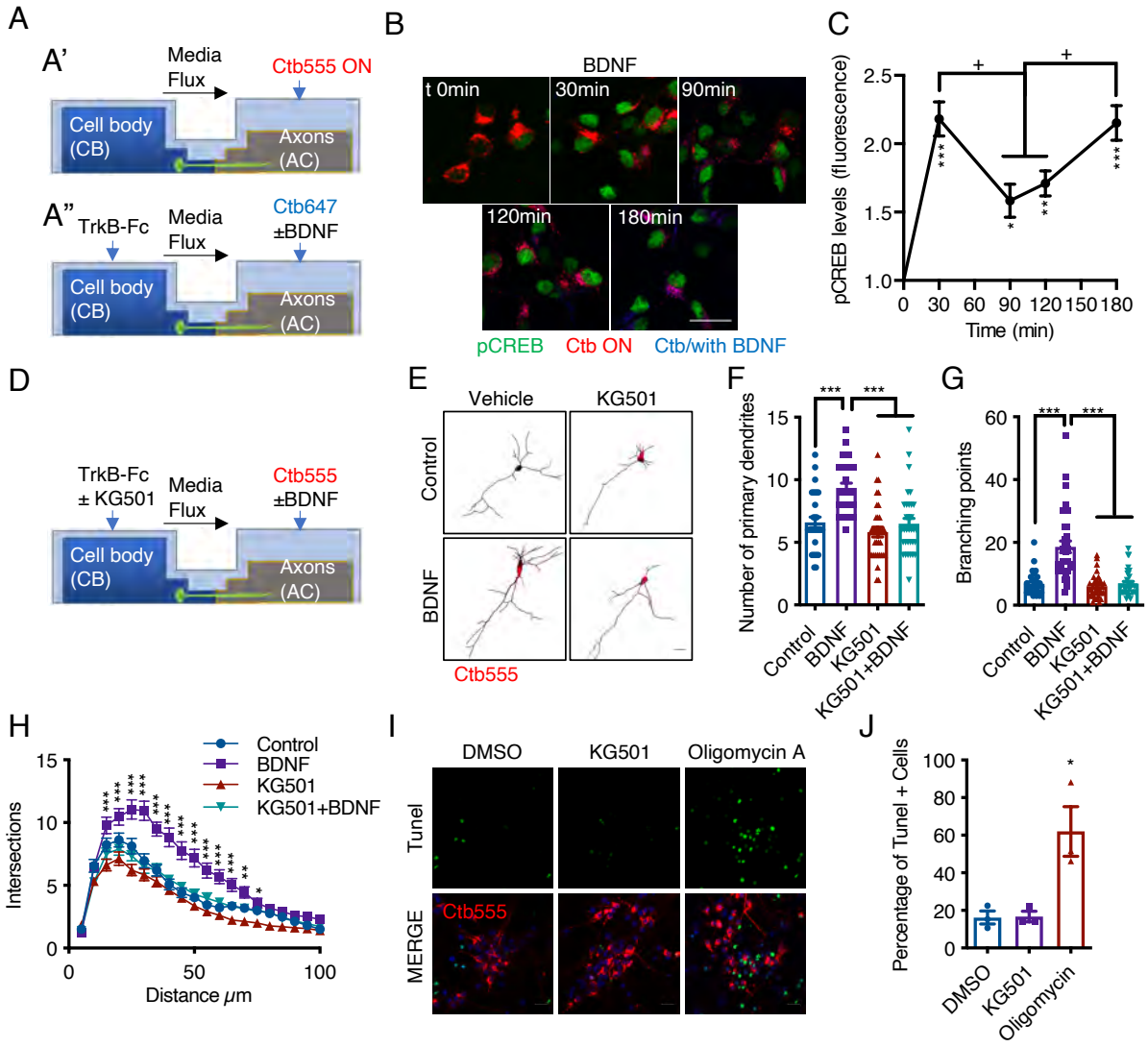
A
A'
Media Flux
Ctb555 ON
Cell body (CB)
Axons (AC)
A"
TrkB-Fc
Media Flux
Ctb647 ±BDNF
Cell body (CB)
Axons (AC)
B
BDNF
t 0min
30min
90min
120min
180min
pCREB
Ctb ON
Ctb/with BDNF
C
pCREB levels (fluorescence)
Time (min)
D
TrkB-Fc ± KG501
Media Flux
Ctb555 ±BDNF
Cell body (CB)
Axons (AC)
E
Vehicle
KG501
Control
BDNF
Ctb555
F
Number of primary dendrites
Control
BDNF
KG501
KG501+BDNF
G
Branching points
Control
BDNF
KG501
KG501+BDNF
H
Control
BDNF
KG501
KG501+BDNF
Intersections
Distance μm
I
DMSO
KG501
Oligomycin A
Tunel
MERGE
Ctb555
J
Percentage of Tunel + Cells
DMSO
KG501
Oligomycin

Figure 3. CREB activity is required for axonal BDNF induced long-distance dendritic arborization. (A) Schematic representation of the protocol to evaluate CREB phosphorylation induced by axonal BDNF. Five DIV cortical neurons were retrograde labeled with Ctb555 (in red) overnight (A'). Next, the culture medium was changed to serum-free medium for 90 minutes and stimulated with BDNF (50 ng/mL) for 5, 30, 90, 120 and 180 minutes along with Ctb647 (in blue) in the axons (A"). Finally, the cultures were fixed and activated CREB was visualized by phospho CREB (pCREB, S133) immunofluorescence performed in CB. **(B)** Representative figures of nuclear pCREB immunostaining in control neurons and stimulated with BDNF in axons for different times points as indicated in A. Scale bar 10 µm. **(C)** Quantification of fluorescence (arbitrary units, A.U) of pCREB in the nucleus in the presence or absence of BDNF. Just neurons positive for Ctb555 were included in the analysis. n= 30-40 neurons from 2 independent experiment. *$p<0.05$, **$p< 0.01$, ***$p< 0.01$ vs control; + $p<0.05$ vs BDNF 90 and 120 min. Results are expressed as ± SEM. Statistics was done by one-way ANOVA test followed by Bonferroni post-test for multiple comparisons. **(D)** Experimental design to study the requirement of CREB activation for axonal BDNF-induced dendritic arborization. The CB was incubated with TrkB-Fc (100 ng/mL) and KG501 (10 µM) for 1 hour. Then, the AC was stimulated with BDNF (50 ng/mL) for 48 hours in the presence of Ctb555 in the axons in the presence or absence of KG501 in the CB. Finally, neurons were fixed and immunofluorescence was performed against MAP2. **(E)** Representative images of neurons in the CB (red indicate Ctb555) from compartmentalized cultures treated with DMSO (control), KG501, BDNF or BDNF in the presence of KG501 CB. Scale bar 20 µm. **(E-H)** Quantification of primary dendrites **(F)**, branching points **(G),** Sholl analysis **(H)**, from neurons labeled with EGFP/MAP2/Ctb555 in each experimental condition. n= 30-35 neurons from 3 independent experiment. *$p<0.05$, **$p< 0.01$, ***$p< 0.001$. Statistics was done by one-way ANOVA test followed by Bonferroni post-test for multiple comparisons (F and G). Two-way ANOVA with Bonferroni post-test for multiple comparisons was used for Sholl analysis. Results are expressed as ± SEM.**(I)** To control for cell death induced by the KG501 drug, we performed experiments as indicated in D by after fixation cell were staining for DNA fragmentation using Tunel (in green). Just neurons labeled with Ctb555 were considered. As a positive control, Oligomycin (10 µM) treatments as indicated in methods, were used. **(J)** Quantification of Tunel positive cells. Scale bar 20 µm. n=2 chambers per condition from 3 independent experiments. *$p=0.05$. Results are expressed as ± SEM. Statistics were done by one-way ANOVA test followed by Bonferroni post-test for multiple comparisons.

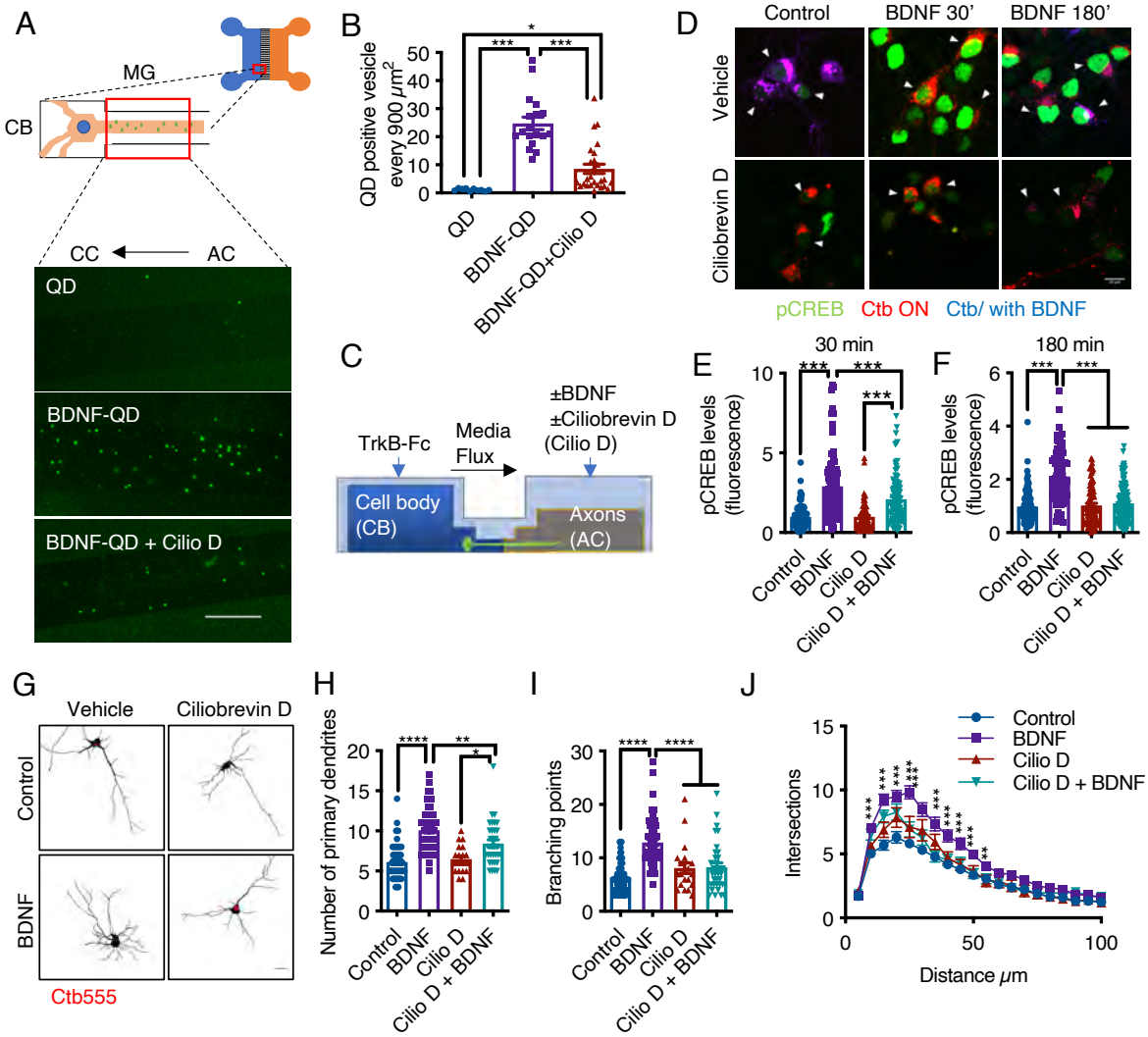
A
MG
CB
CC
AC
QD
BDNF-QD
BDNF-QD + Cilio D
B
QD positive vesicle every 900 μm2
QD
BDNF-QD
BDNF-QD+Cilio D
C
TrkB-Fc
Media Flux
±BDNF
±Ciliobrevin D
(Cilio D)
Cell body (CB)
Axons (AC)
D
Control
BDNF 30'
BDNF 180'
Vehicle
Ciliobrevin D
pCREB
Ctb ON
Ctb/ with BDNF
E
30 min
pCREB levels (fluorescence)
Control
BDNF
Cilio D
Cilio D + BDNF
F
180 min
G
Vehicle
Ciliobrevin D
Control
BDNF
Ctb555
H
Number of primary dendrites
I
Branching points
J
Control
BDNF
Cilio D
Cilio D + BDNF
Intersections
Distance μm

Figure 4. Dynein activity is required for phosphorylation of CREB and dendritic arborization induced by BDNF. (A) Schematic representation of the protocol to evaluate retrograde transport of BDNF. Biotinylated BDNF conjugated to Streptavidin quantum dot 655 (QD) (2 nM) was incubated in the AC for 4 hrs in the presence or absence of Ciliobrevin D (20 µM). Then, after washed, neurons were fixed, and the accumulation of BDNF-QD was evaluated in the proximal compartment of the microgrooves (MG). As a control, non-conjugated QDs were used. Representative images of BDNF-QD (dots in green) of the proximal region of MG in each condition. **(B)** Quantification of QD positive vesicles in the proximal region of MG every 900 µm per each condition. Scale bar 10 µm. N= 36 microgrooves from 3 independent experiments were analyzed. **(C)** Experimental design to study dynein dependent axonal BDNF signaling in compartmentalized cortical neurons. Five DIV cortical neurons were retrogradely labeled with Ctb555 (in red) over-night. The next day, the culture medium was changed to serum-free medium for 90 minutes in the presence or absence of Ciliobrevin D in the AC. Then, AC was stimulated with BDNF (50 ng/mL) for 30, and 180 minutes along with Ctb647 (in blue) in the axon in the presence or absence of Ciliobrevin D. Finally, the cultures were fixed and phosphoCREB (pCREB, S133) was visualized by immunofluorescence. **(D)** Representative images of nuclear pCREB in neurons stimulated or non-stimulated with BDNF, Ctb555 (in red), and Ctb647(in blue) added to axons in the presence or absence of axonal Ciliobrevin D. Scale bar 10 µm. **(E-F)** Quantification of the fluorescence (Arbitrary Units, A.U.) associated with pCREB immunostaining in the nucleus of neurons labeled with Ctb555 and stimulated with BDNF during 30 minutes (E) or 180 min (F). n= 83-111 neurons from 3 independent experiment. **(G)** Six DIV cortical neurons were transfected with EGFP, then the CB was treated with TrkB-Fc (100 ng/mL), and the AC was treated with Ctb555 and BDNF (50 ng/mL) with or without Ciliobrevin D (20 µM) for 48 hours. Finally, neurons were fixed, and immunofluorescence was performed against MAP2. Representative images of the neuronal morphology of neurons labeled with Ctb555 (in red) and treated in the AC during 48 hours from compartmentalized cultures with DMSO (control), Ciliobrevin D, BDNF or BDNF and pretreated with Ciliobrevin D. **(H-J)** Quantification of primary dendrites **(H)**, branching points **(I),** Sholl analysis **(J)**, from neurons labeled with EGFP/MAP2/Ctb555 in each experimental condition as indicated in G. Scale bar 20 µm. n= 34-65 neurons from 3 independent experiment. *$p<0.05$, **$p< 0.01$, ***$p< 0.001$, ****$p<0.0001$. Results are expressed as ± SEM. Statistics were done by one-way ANOVA test and Bonferroni post-test for multiple comparisons (E, F, H, and I). Statistical comparison of the Sholl analysis was made by two-way ANOVA with Bonferroni posthoc test for multiple comparisons.

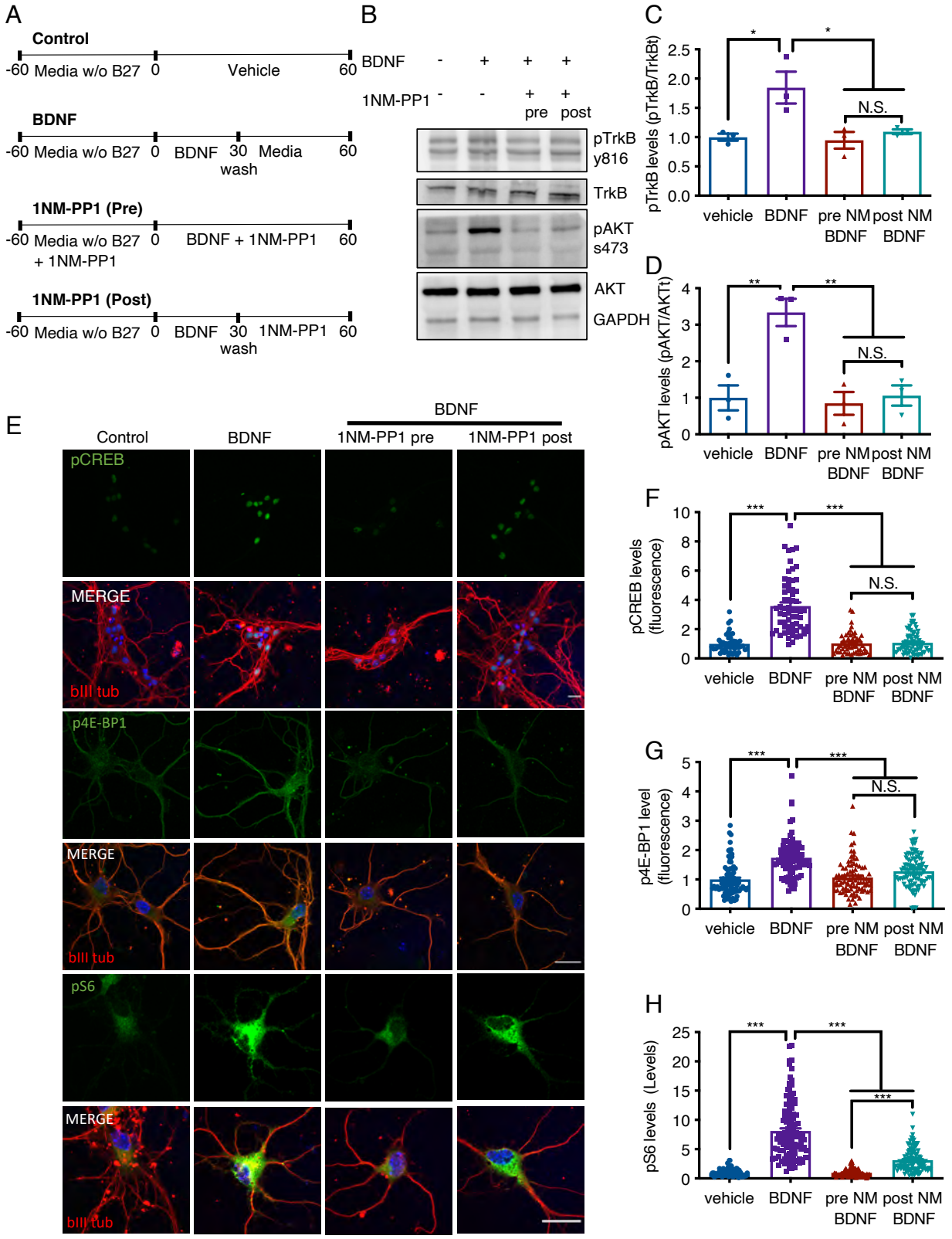
A
Control
-60 Media w/o B27 0 Vehicle 60
BDNF
-60 Media w/o B27 0 BDNF 30 Media wash 60
1NM-PP1 (Pre)
-60 Media w/o B27 + 1NM-PP1 0 BDNF + 1NM-PP1 60
1NM-PP1 (Post)
-60 Media w/o B27 0 BDNF 30 1NM-PP1 wash 60
B
BDNF - + + +
1NM-PP1 - - + + pre post
pTrkB y816
TrkB
pAKT s473
AKT
GAPDH
C
pTrkB levels (pTrkB/TrkBt)
vehicle BDNF pre NM BDNF post NM BDNF
N.S.
D
pAKT levels (pAKT/AKTt)
N.S.
E
Control BDNF BDNF 1NM-PP1 pre 1NM-PP1 post
pCREB
MERGE
bIII tub
p4E-BP1
pS6
F
pCREB levels (fluorescence)
G
p4E-BP1 level (fluorescence)
H
pS6 levels (Levels)

Figure 5. 1NM-PP1 is able to reduce TrkB activation, after BDNF treatment, in TrkB^{F616A} cortical neurons. (A) Diagrams of the experimental designs used for stimulating neurons in non-compartmentalized cultures. 7 DIV cortical neurons were depleted from media during 1 hour in the presence or absence of 1NM-PP1 (1 μM). Then neurons were treated as follow: control: vehicle 1 hour. BDNF: incubation of BDNF (50 ng/mL) for 30 minutes, next were rinse twice and incubated with vehicle. 1NM-PP1 (Pre): incubation with BDNF in the presence of 1NM-PP1 for 1 hour. 1NM-PP1 (Post): incubation with BDNF for 30 minutes, next were rinse twice and incubated with 1NM-PP1 for 30 minutes. **(B)** Immunoblot of pTrkB (Y816), TrkB, pAkt (S437), Akt and GAPDH from cortical neurons stimulated as indicated in A. **(C)** Quantification of pTrkB levels normalized with total TrkB. **(D)** Quantification of pAkt levels normalized with total Akt. n=3 independent experiments. **(E)** Representative image of cortical neurons treated as indicated in A. In green is shown pCREB, p4E-BP1 or pS6, in red is shown bIII tubulin. **(F)** Quantification of fluorescence (arbitrary units, A.U) of pCREB in the nucleus of neurons. **(G)** Quantification of fluorescence (arbitrary units, A.U) of p4E-BP1 in the primary dendrites. **(H)** Quantification of fluorescence (arbitrary units, A.U) of pS6 in primary dendrites. n=49-72 neurons from 3 independent experiments. Results are expressed as ± SEM. *$p< 0.05$; **$p<0.01$; ***$p< 0.001$. Statistics was done by one-way ANOVA test followed by Bonferroni post-test for multiple comparisons.

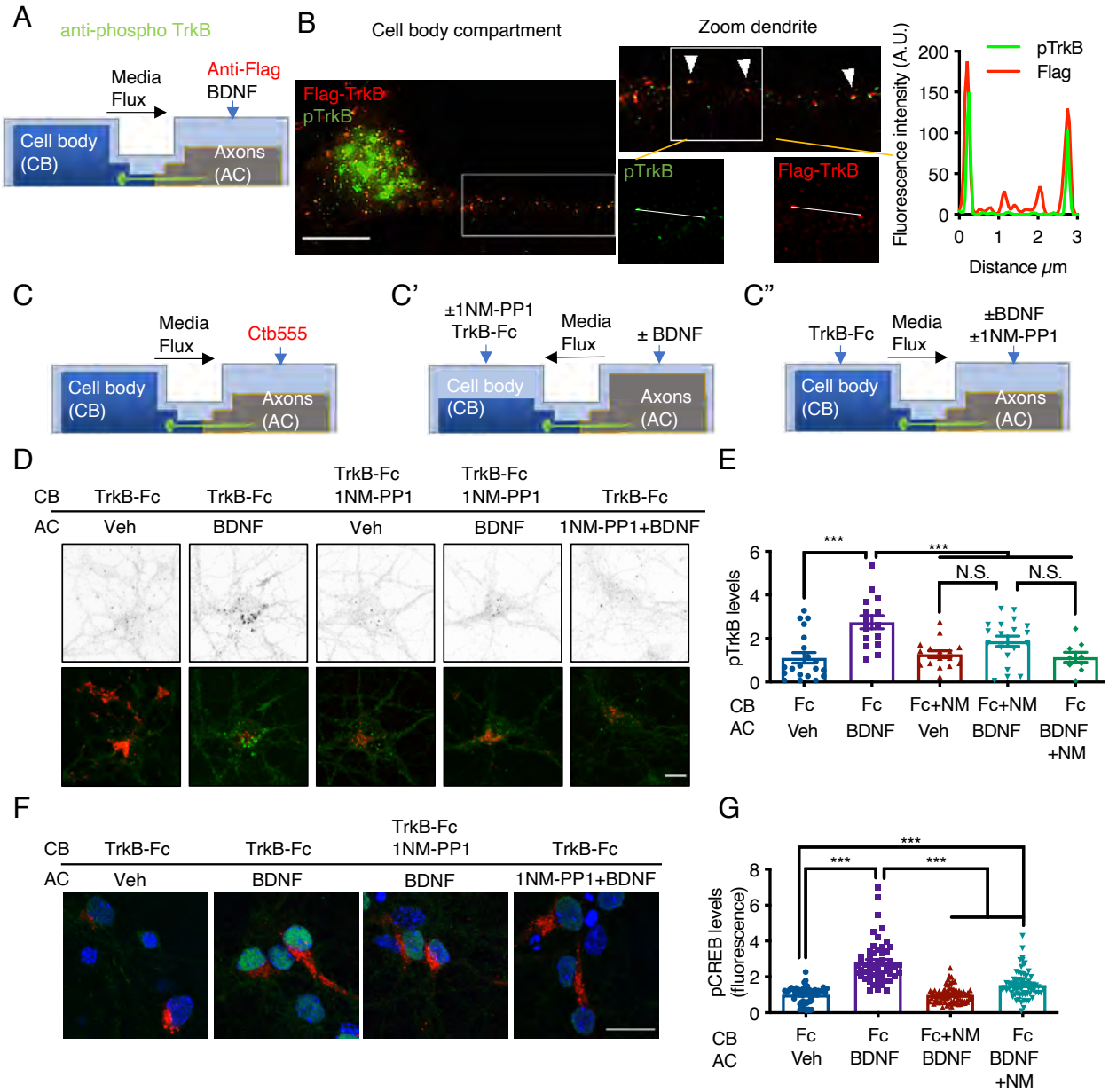
A
anti-phospho TrkB
Media
Flux
Anti-Flag
BDNF
Cell body
(CB)
Axons
(AC)
B
Cell body compartment
Flag-TrkB
pTrkB
Zoom dendrite
pTrkB
Flag-TrkB
Fluorescence intensity (A.U.)
200
150
100
50
0
0
1
2
3
Distance μm
pTrkB
Flag
C
Media
Flux
Ctb555
Cell body
(CB)
Axons
(AC)
C'
±1NM-PP1
TrkB-Fc
Media
Flux
± BDNF
Cell body
(CB)
Axons
(AC)
C"
TrkB-Fc
Media
Flux
±BDNF
±1NM-PP1
Cell body
(CB)
Axons
(AC)
D
CB
AC
TrkB-Fc
Veh
TrkB-Fc
BDNF
TrkB-Fc
1NM-PP1
Veh
TrkB-Fc
1NM-PP1
BDNF
TrkB-Fc
1NM-PP1+BDNF
E
pTrkB levels
6
4
2
0
***
***
N.S.
N.S.
CB
AC
Fc
Veh
Fc
BDNF
Fc+NM
Veh
Fc+NM
BDNF
Fc
BDNF
+NM
F
CB
AC
TrkB-Fc
Veh
TrkB-Fc
BDNF
TrkB-Fc
1NM-PP1
BDNF
TrkB-Fc
1NM-PP1+BDNF
G
pCREB levels
(fluorescence)
8
6
4
2
0
***
***
***
CB
AC
Fc
Veh
Fc
BDNF
Fc+NM
BDNF
Fc
BDNF
+NM

Figure 6. Somatodendritic activity of axonal TrkB is required for BDNF long-distance signaling of BDNF. (A) Schematic representation of the protocol used to label axonal TrkB. Five DIV compartmentalized cortical neurons were transfected with Flag-TrkB for 48 hrs. At DIV seven, the axonal compartment was incubated with anti-Flag antibodies for 40 min at 4ºC. Then, neurons were incubated at 37°C in the presence and absence of BDNF (50 ng/mL). Finally, immunofluorescence was performed against phosphorylated TrkB (Y816, pTrkB) (in green) and anti-Flag (in red). **(B)** Immunofluorescence of pTrkB and internalized Flag-TrkB in compartmentalized neurons treated with BDNF in the axons as shown in A. Representative images of neuron in BDNF condition in cell body compartment. In the right panel, a zoom of a proximal dendrite of the neurons shown in the left panel. The arrows indicate the co- colocalization of Flag (in red) and pTrkB (in green). Scale bar 5 µm. At right, graphs showing the fluorescence intensity profile pixel by pixel on the white lines shown in the right panels in B. Green line indicates the fluorescent profile of the pTrkB-associated fluorescence and the red lines indicate the fluorescent profile of the Flag-TrkB associated fluorescence. **(C-C'')** Schematic representation of the protocol used for stimulating neurons. **(C)** At 6 DIV AC of cortical neurons from $TrkB^{F616A}$ was incubated with Ctb555 overnight. Next day (7 DIV) there was two types of treatments: (C') Neurons were depleted of B27 supplement during 1 hour in the presence of 1NM-PP1 (1 µM) in the CB, with the flux toward the CB. Then, the CB was treated with TrkB-Fc (100 ng/mL) with 1NM-PP1 and the AC was treated with or without BDNF (50 ng/mL) for 3 hours. (C'') Neurons were depleted of B27 supplement during 1 hour in the presence or absence of 1NM-PP1 (1 µM) in the AC, with the flux toward the AC. Then the CB was treated with TrkB-Fc, and the AC was incubated with or without BDNF in the presence or absence of 1NM-PP1 for 3 hours. Finally, neurons were fixed and an immunofluorescence against phosphor-TrkB (pTrkB, Y816) or phosphor-CREB (pCREB, S133) was performed. **(D)** Representative images of pTrkB in the CB compartment of Ctb positive neurons treated as described in A. **(E)** Quantification of pTrkB levels in the cell body of each treatment as indicated in B. n=3 independent experiment. **(F)** Representative image of cortical neurons immunostained for pCREB stimulated with BDNF in the axonal compartment for 3 hrs in the presence or absence of 1NM-PP1 in the CB (1NM- PP1/BDNF) or AC (1NM-PP1 + 1NM-PP1) respectively. **(G)** Quantification of pCREB levels in Ctb positive neurons of each condition. n= 78-86 neurons from 3 independent experiment. **$p< 0.01$, ***$p<0.001$. vs control. Results are expressed as ± SEM. Statistics was done by one-way ANOVA test and Bonferroni post-test for multiple comparisons.

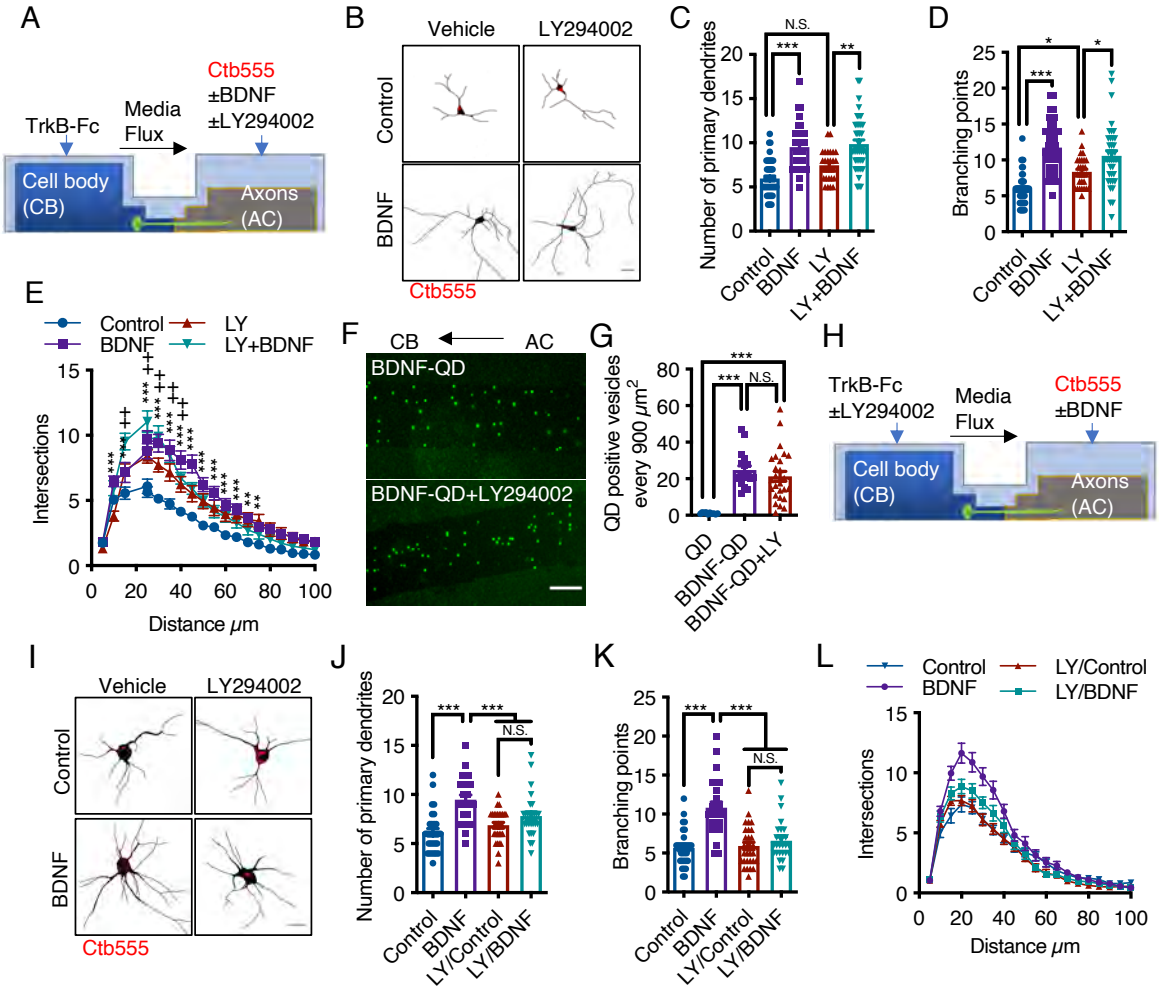
A
TrkB-Fc
Media Flux
Ctb555 ±BDNF ±LY294002
Cell body (CB)
Axons (AC)
B
Vehicle
LY294002
Control
BDNF
Ctb555
C
Number of primary dendrites
N.S.
***
**
Control
BDNF
LY
LY+BDNF
D
Branching points
*
***
*
E
Control
BDNF
LY
LY+BDNF
Intersections
Distance μm
F
CB
AC
BDNF-QD
BDNF-QD+LY294002
G
QD positive vesicles every 900 μm²
***
N.S.
QD
BDNF-QD
BDNF-QD+LY
H
TrkB-Fc ±LY294002
Media Flux
Ctb555 ±BDNF
Cell body (CB)
Axons (AC)
I
Vehicle
LY294002
Control
BDNF
Ctb555
J
Number of primary dendrites
LY/Control
LY/BDNF
K
Branching points
L
Control
BDNF
LY/Control
LY/BDNF
Intersections
Distance μm

Figure 7. Activation of PI3K activity in the cell bodies and not in the axons (AC) was required for dendritic arborization induced by axonal BDNF. (A) Schematic representation of the protocol to stimulate compartmentalized cortical neurons. Six DIV cortical neurons were transfected with EGFP, then the CB was treated with TrkB-Fc (100 ng/mL) and the AC was treated with Ctb555 and BDNF (50 ng/mL) with or without LY294002 (10 µM) during 48 hours. Finally, neurons were fixed and immunofluorescence was performed against MAP2. **(B)** Representative images of neurons in the CB (red indicated Ctb555) from compartmentalized cultures treated with DMSO in the presence or absence of BDNF and LY294002 in AC. **(C-E)** Quantification of primary dendrites **(C)**, branching points **(D),** and Sholl analysis **(E)**, from neurons labelled with EGFP/MAP2/Ctb555 in the different experimental conditions as described in B. Scale bar 20 µm. n= 29-48 neurons from 3 independent experiment. **(F)** The Ac was treated with 2 nM of BDNF-QD for 4 hours in the presence or absence of LY294002 (10 µM) to promote the retrograde transport of BDNF. Then, neurons were fixed and the accumulation of BDNF-QD was evaluated in the proximal compartment of the microgrooves (MG). Representative image of BDNF-QD (in green dots) accumulation in the proximal part of MG in each treatment. Scale bar 10 µm. **(G)** Quantification of QD positive vesicles in the proximal region of MG every 900 µm per each condition. Scale bar 10 µm. N= 36 microgrooves from 3 independent experiment were analyzed. **(H)** Schematic representation of the protocol to stimulate compartmentalized cortical neurons. Six DIV cortical neurons were transfected with EGFP, then the CB was treated with TrkB-Fc (100 ng/mL) in the presence or absence of LY294002 (10 µM) and the AC was treated with Ctb555 and BDNF (50 ng/mL) during 48 hours. Finally, neurons were fixed and immunofluorescence was performed against MAP2. **(I)** Representative images of neurons in the CB (red indicated Ctb555) from compartmentalized cultures treated in the CB with DMSO (control) or LY294002 and in the AC with or without BDNF. Scale bar 20 µm. **(C-E)** Quantification of primary dendrites **(C)**, branching points **(D),** Sholl analysis **(E)**, from neurons labelled with EGFP/MAP2/Ctb555. n= 25-30 neurons from 3 independent experiment. *$p<0.05$, **$p< 0.01$, ***$p< 0.001$, +$p<0.05$ LY294002 vs LY294022/BDNF. Results are expressed as ± SEM. Statistics was done by one-way ANOVA test and Bonferroni post-test for multiple comparisons (C, D, G, J, and K). Statistical comparison of the Sholl´s analysis was done by two-way ANOVA with Bonferroni post-hoc test for multiple comparisons.

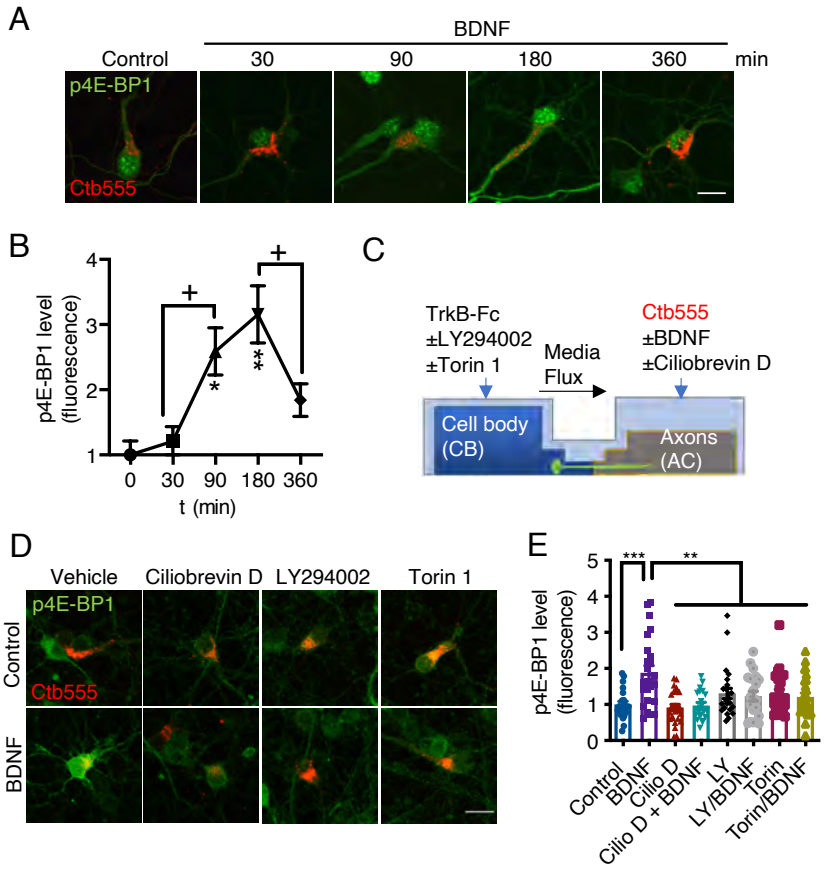

Figure 8. Axonal BDNF promotes mTOR activation in the cell body of compartmentalized cortical neurons in a PI3K-dependent manner. (A) Representative images of phosphorylated 4E-BP1 (p4E-BP1) immunostaining (in green) and Ctb555 (in red). Six DIV compartmentalized cortical neurons were incubated with Ctb555 overnight. At 7 DIV, neurons were treated in the axonal compartment with BDNF (50 ng/mL) during 30, 60, 180 or 360 minutes. **(B)** Time-course quantification of somatodendritic p4E-BP1 associated immunofluorescence in primary dendrites. **(C)** Schematic representation of the protocol used to evaluate the effect of different pharmacological inhibitors on the axonal BDNF-induced phosphorylation of 4E-BP1 in cell bodies. Six DIV cortical neurons were pretreated with DMSO (control), LY294002 (10 µm; LY), Torin 1 (0.25 µm; Torin) in the CB compartment or Ciliobrevin D (20 µm; Cilio D) in the AC for 1 hour. Then, BDNF was added during 180 minutes in the AC in the presence or absence of these inhibitors. **(D)** Representative images of p4E-BP1 (in green) in somatodendritic compartment of neurons stimulated with BDNF, in the presence or absence of different inhibitors. **(E)** Quantification of somatodendritic p4E-BP1 in each treatment of neurons labeled with Ctb555 (in red). Scale bar 20 µm. n= 31-36 neurons from 3 independent experiment. *p<0.05, **p< 0.01, ***p< 0.001. vs control; +p<0.05 vs BDNF 90 and 360 min in B. Results are expressed as ± SEM. Statistics was done by one-way ANOVA test and Bonferroni post-test for multiple comparisons.

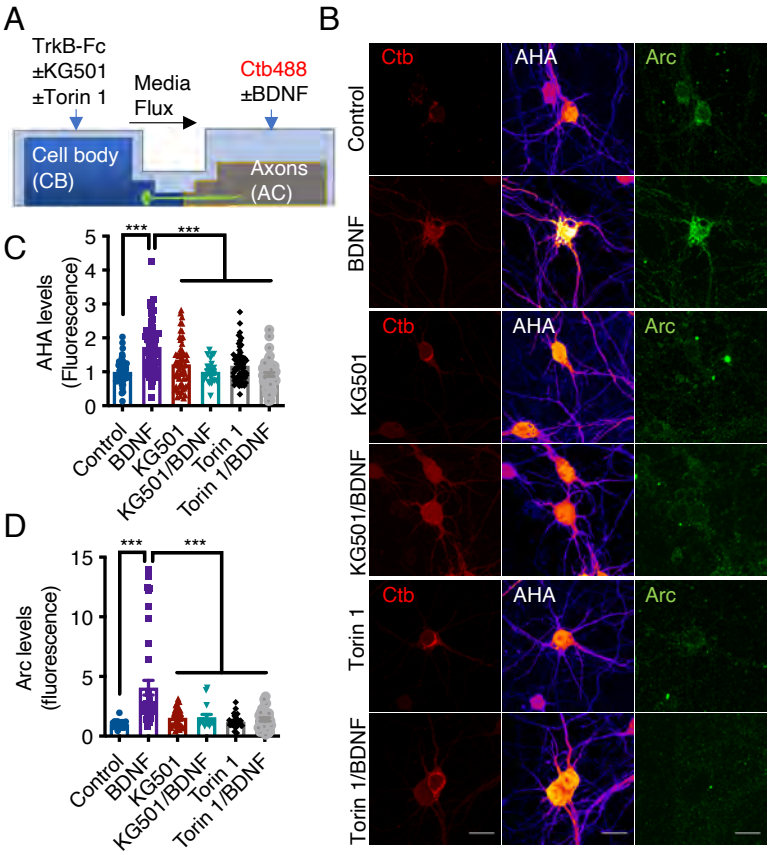

Figure 9. Axonal BDNF promotes somatodendritic protein synthesis in a mTOR and CREB dependent manner. **(A)** Schematic representation of the protocol to evaluate protein synthesis. Six-7 DIV cortical neurons were incubated in free methionine media during 1 hour in the presence or absence of KG501 (10 µm) or Torin 1 (0.25 µm) in the CB. Then, both the CB and AC were incubated with AHA, but just the axonal compartment was stimulated with BDNF (50 ng/mL) in the presence of Ctb488 during 5 hours. **(B)** Representative images of neurons positive for Ctb488, AHA staining and Arc immunofluorescence of control condition and stimulated with BDNF, in the presence or absence of KG501 and Torin 1. **(C)** Quantification of AHA fluorescence in the primary dendrite of neurons labeled with Ctb488 in each different treatment. **(D)** Quantification of Arc fluorescence in the somas of neurons labelled with Ctb488 in each different treatment. Scale bar 20 µm. n= 30-48 neurons from 3 independent experiment. ***p< 0.001. Statistics was done by one-way ANOVA test and Bonferroni post-test for multiple comparisons.